

# DESIGN REPORT

Autonomous Aerial Vehicle Challenge  
(AAVC 2021-2022)



YEUN TUM OUPRAKORN TEAM

Department of Aerospace Engineering

Kasetsart University

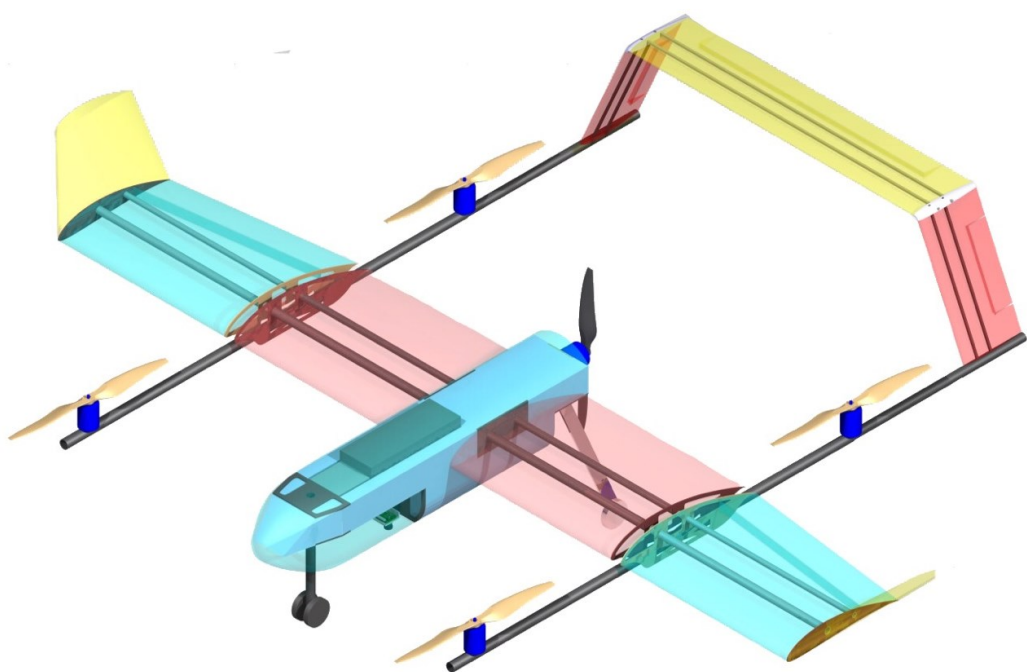




## Table of Contents

<b>1.0</b>	<b>Executive Summary.....</b>	<b>6</b>
<b>1.1</b>	<b>UAV Design-Process MAP.....</b>	<b>8</b>
<b>2.0</b>	<b>Team Organization.....</b>	<b>9</b>
<b>2.1</b>	<b>Project Milestone Chart.....</b>	<b>10</b>
<b>3.0</b>	<b>Conceptual Development.....</b>	<b>11</b>
<b>3.1.2</b>	<b>Hybrid Total Mission Score.....</b>	<b>12</b>
<b>3.2</b>	<b>Sensitivities Matrix.....</b>	<b>13</b>
<b>3.4</b>	<b>Conceptual Design Selection .....</b>	<b>14</b>
<b>3.4.1</b>	<b>UAV Configuration Selection.....</b>	<b>15</b>
<b>3.4.3</b>	<b>Landing Gear Configuration Selection .....</b>	<b>16</b>
<b>3.4.4</b>	<b>Propeller Configuration and Location Selection .....</b>	<b>16</b>
<b>3.4.5</b>	<b>Tail Configuration.....</b>	<b>17</b>
<b>3.5.1</b>	<b>Wing Sizing.....</b>	<b>19</b>
<b>3.5.2</b>	<b>Horizontal Tail Sizing.....</b>	<b>20</b>
<b>3.5.3</b>	<b>Vertical Tail Sizing .....</b>	<b>20</b>
<b>3.6</b>	<b>Drag Estimation.....</b>	<b>21</b>
<b>3.7</b>	<b>Motor and Battery Selection.....</b>	<b>25</b>
<b>4.0</b>	<b>Preliminary and Detailed design .....</b>	<b>28</b>
<b>4.1</b>	<b>Aerodynamic Analysis .....</b>	<b>28</b>
<b>4.1.1</b>	<b>Aerodynamics prediction.....</b>	<b>28</b>
<b>4.1.2</b>	<b>Airfoil Selection.....</b>	<b>29</b>
<b>4.3</b>	<b>Structural Analysis.....</b>	<b>30</b>
<b>4.3.1</b>	<b>Aero Lift.....</b>	<b>31</b>
<b>4.3.2</b>	<b>Load Distribution.....</b>	<b>31</b>
<b>4.3.3</b>	<b>Shear Force &amp; Bending Moment Diagram.....</b>	<b>32</b>
<b>4.3.4</b>	<b>Position and Sizing of Spar.....</b>	<b>33</b>
<b>4.4</b>	<b>Stability Analysis .....</b>	<b>36</b>
<b>4.4.1</b>	<b>Static Stability.....</b>	<b>36</b>
<b>4.4.2</b>	<b>Dynamic Stability .....</b>	<b>39</b>
<b>4.5.1</b>	<b>Antenna Tracker Hardware.....</b>	<b>43</b>
<b>4.5.2</b>	<b>Antenna Tracker Assembly .....</b>	<b>45</b>
<b>4.6</b>	<b>Image Processing.....</b>	<b>45</b>
<b>4.6.1</b>	<b>Composition of Imagery System.....</b>	<b>45</b>
<b>4.6.2</b>	<b>System Schematic.....</b>	<b>46</b>



<b>4.6.3 Camera</b> .....	46
<b>4.6.4 Camera Mount &amp; Servo</b> .....	48
<b>4.6.5 GPS Receiver</b> .....	49
<b>4.6.6 Microprocessor</b> .....	49
<b>4.6.7 Wirings</b> .....	51
<b>4.6.8 Antennae</b> .....	52
<b>4.6.9 Software</b> .....	52
<b>5.0 Manufacturing</b> .....	53
<b>5.1 Material and Fabrication method selection</b> .....	53
<b>5.1.1 Fuselage</b> .....	53
<b>5.1.2 Wing and Empennage</b> .....	54
<b>5.1.3 Landing gear</b> .....	55
<b>5.1.4 Imagery system</b> .....	56
<b>5.1.5 Payload system</b> .....	56
<b>5.2 Manufacturing Plan</b> .....	57
<b>5.3 Project Cost Breakdown Structure</b> .....	58
<b>6.0 Testing Plan</b> .....	60
<b>6.1 Testing objective and testing method</b> .....	60
<b>6.1.1 Propulsion and Control system</b> .....	60
<b>6.1.2 Wing and Spar</b> .....	61
<b>6.1.3 Landing Gear</b> .....	61
<b>6.1.4 Payload Drop System</b> .....	61
<b>6.1.5 Performance</b> .....	61
<b>6.2 Flight Test Schedule</b> .....	61
<b>6.3 Pre-flight Checklist</b> .....	62
<b>7.0 Appendix</b> .....	63



## List of Figures

Figure 1 : UAV Design Process.....	8
Figure 2 : Team Organization.....	9
Figure 3 : Overview of Operating Area .....	11
Figure 4 : Score Ratio.....	13
Figure 5 : Wing Dimension (Top View).....	19
Figure 6 : Wing Dimension (Front View) .....	19
Figure 7 : Horizontal Tail Dimension (Top View).....	20
Figure 8 : Vertical Tail Dimension .....	20
Figure 9 : CFD Analysis.....	22
Figure 10 : Approximated Wetted of Motor Assembly, Front View (Unit mm).....	22
Figure 11 : Drag Coefficient for Other Shape .....	23
Figure 12 : Maching Chart .....	25
Figure 13 : Force on Aircraft in Level flight.....	26
Figure 14 : Baterry 16000 mAh.....	27
Figure 15 : Cl/Cd VS Alpha .....	28
Figure 16 : CI VS Alpha and Cd VS Alpha .....	28
Figure 17 : CI VS Cd and Cm VS Alpha.....	29
Figure 18 : 0012 Airfoil.....	29
Figure 19 : MH 113 Airfoil .....	29
Figure 20 : MH 113 Airrfoil .....	30
Figure 21 : Lift Coefficient VS Span Plot .....	30
Figure 22 : Shear Diagram.....	33
Figure 23 : Bending Diagram.....	33
Figure 24 : Wing Semi Span .....	34
Figure 25 : Moment of Wing Spar .....	35
Figure 26 : Hollow Carbon Fiber Cylindrical .....	36
Figure 27 : Pitching Moment and Angle of Attack .....	37
Figure 28 : Center of Gravity Position.....	37
Figure 29 : Rolling Moment and Sideslip Angle .....	38
Figure 30 : Yawing Moment and Sideslip Angle.....	39
Figure 31 : Flight Dynamic Reference Frame .....	39
Figure 32 : Longitudinal Stability Root Locus .....	41
Figure 33 : Lateral Directional Stability Root Locus.....	42
Figure 34 : Flat Patch Antenna .....	43
Figure 35 : Radio Frequency (RF) Antenna Gain Patterns.....	43
Figure 36 : Controller Pixhawk .....	43
Figure 37 : GPS Module.....	44
Figure 38 : Servo.....	44
Figure 39 : Long-Range Telemetry Module.....	44
Figure 40 : Antenna Tracker and Telemetry Configuration.....	45
Figure 41 : Camera Bay Assembly, Microprocessor Units Located Abrove Fulage Frame .....	45
Figure 42 : Image Processing Configuration.....	46
Figure 43 : Arducam 12MP HQ Camera, Isometric.....	46
Figure 44 : Front View .....	46
Figure 45 : Back View .....	47



Figure 46 : Camera Specification .....	48
Figure 47 : Camera Assembly, Arrow Indicates Direction Towards Nose of The Aircraft .....	48
Figure 48 : Digital Servo Actuators.....	49
Figure 49 : GPS Receiver Module.....	49
Figure 50 : Raspberry Pi Microprocessor, Isometric.....	49
Figure 51 : Top View.....	50
Figure 52 : Mechanical Drawing .....	50
Figure 53 : Microprocessor Specifications.....	51
Figure 54 : Ribbon Cables.....	51
Figure 55 : Aomway Antenna.....	52
Figure 56 : Fuselage Model.....	53
Figure 57 : Main Fuselage Structure.....	53
Figure 58 : Aerodynamic Faring.....	54
Figure 59 : Twin-Boom Inverted U-Tail.....	54
Figure 60 : Wing .....	55
Figure 61 : Plywood Rib Part.....	55
Figure 62 : Camera Assembly.....	56
Figure 63 : Payload System.....	56



## List of Tables

Table 1 : Project Milestone.....	10
Table 2 : Requirement.....	11
Table 3 : Mission Score .....	12
Table 4 : Autonomy Level Factor .....	12
Table 5 : Mission Requirements and Solution .....	14
Table 6 : Aircraft Configuration Selection.....	15
Table 7 : Wing Location Configuration Selection .....	16
Table 8 : Landing Gear Configuration Selection .....	16
Table 9 : Propeller Configuration and Location Selection.....	17
Table 10 : Tail Configuration Selection.....	18
Table 11 : Wing Configuration.....	19
Table 12 : Horizontal Tail Configuration .....	20
Table 13 : Vertical Tail Configuration .....	21
Table 14 : Motor Specification .....	26
Table 15 : VTOL Motor Specification .....	27
Table 16 : UAV Configuration .....	30
Table 17 : Dead Weight.....	31
Table 18 : Aero Lift.....	32
Table 19 : Load Distribution.....	32
Table 20 : Spar Moment of Inertia .....	35
Table 21 : Hollow Circular Spar Moment of Inertia.....	36
Table 22 : Stability Coefficient.....	40
Table 23 : Longitudinal Dynamics Stability Parameters .....	40
Table 24 : Lateral Directional Stability Parameters .....	42
Table 25 : Electrical Specifications .....	43
Table 26 : Camera Capability .....	47
Table 27 : Manufacturing Plan .....	57
Table 28 : Cost Breakdown Structure .....	59
Table 29 : Testing Goal of Each Component in Propulsion and Control System .....	60
Table 30 : Flight Test Schedule .....	62
Table 31 : Pre Flight Checklist .....	62
Table 32 : Cost Estimation.....	64



## 1.0 Executive Summary

This report summarizes design, manufacturing, and testing process of unmanned aerial vehicle use for Autonomous Aerial Vehicle Challenge (AAVC 2021-2022) by Kasetsart University's CiiMAV team. In this competition, our team designed a modular UAV that can be converted into both fix-wing UAV and Hybrid UAV. Subsequently, can be used in track1 (fix-wing) and track3 (hybrid configuration) of the competition. The main mission in the competition is to use the UAV to find escaped experiment subjects and release the payload (tranquillizer bomb) to the target within the effective range.

In this mission, for hybrid wing category, overall mission objectives were identified as follows.

- Set up control station and ready the UAV for launch within 5 minutes.
- UAV shall possess ability to operate autonomously with automatic flight control system ( $f_{auto}$ ).
- Safely take-off from 5x5 m launching pad.
- Accurately drop payload on target within effective range (15m from target).
- Maintain visual contact with the acquired target for 60 seconds.
- The target identification accuracy (overall shape and details of the target)
- Locate and mark targets with GPS coordinates.
- Landing with no damage while maintaining UAV precision related to the launching pad.
- Operation shall be performed within 15 minutes.

Additionally, concerns in regards of the mission payload were defined as follows.

- Payload must possess weight range of 0.5-1 kilograms.
- The payload shape is a cylindrical bottle with approximate dimension of 65mm in diameter and 240mm in length, which can contain pure water. With maximum volume of 450ml, where conventional water bottle with volume of 450ml can be used.

With all mission objective outlined above, the requirements for UAV design can also be defined. The requirements were then used in our UAV design process, as the subsequent design will result in the best combination of performance. We believe that with design based on optimal values will enable us to earn the most point in this competition.

At the beginning of the design process, we start from sketching several conceptual design configurations of the UAV. Comparisons and computational analysis between different configurations were also done to verify characteristics of each configuration, for instance with conventional aft-tail and canard. We use trade-off study to help to select the best configuration that satisfy the mission objectives.

After a devoted trade-off study was done, we select conventional aft-tail configuration due to more flexibility of modifications to the design and the easiest to manufacture. A mid-wing placement was chosen due to superior aerodynamics coupled with merits on weight saving and manufacturability. Meanwhile, twin boom tail configuration was selected due to higher modularity to convert the same airframe to a vertical take-off and landing variant. For



extra protection of the propeller, a single pusher configuration was chosen. Subsequently, to avoid prop wash an inverted U-tail was ultimately chosen.

After our UAV configuration was concluded, preliminary and detailed design analysis was done thoroughly. Calculation and analysis of aerodynamics, stability, and structure were executed. Meanwhile a full-scale CAD model of the UAV was also generated. Moreover, design process also extends to various subsystem of the UAV such as: flight control system, imagery system, antenna tracking system, and other relevant systems. All of which, would facilitate our team to excel in the competition.

For material selection, our team primarily choose lightweight materials for example Styrofoam or composite materials. Composite materials were used in locations where additional strength was required. Moreover, fabrication methods that aid ease of manufacture and repair were chosen to improve development and maintenance speeds.

When manufacturing process concluded, integration and assembly of all parts subsystems of UAV will be done for preliminary testing. After ground test of the UAV was performed and verified, flight tests will be performed along with pilot-aircraft familiarization to prepare for AAVC 2021-2022 competition.



## 1.1 UAV Design-Process MAP

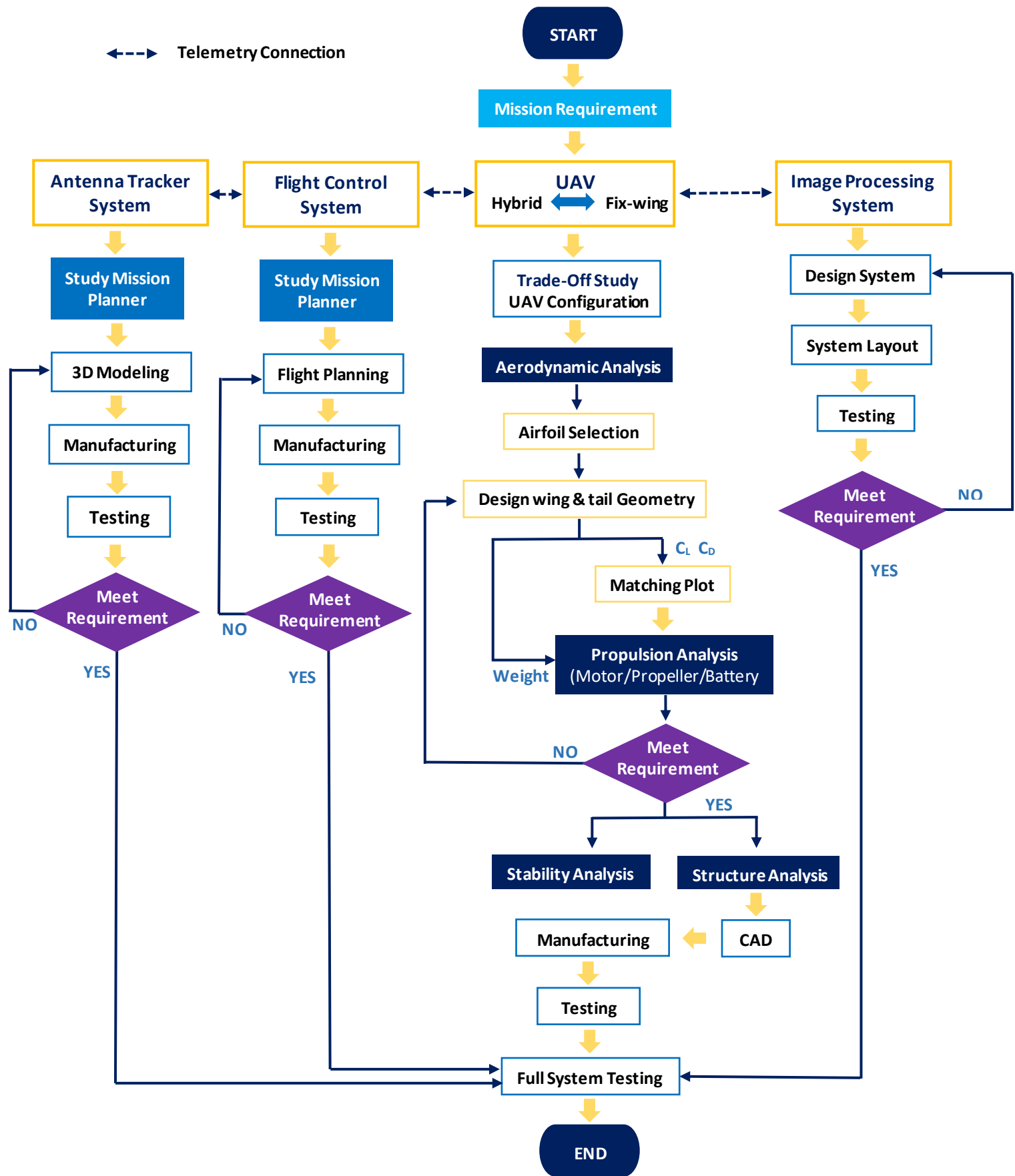


*Figure 1 : UAV Design Process*



## 2.0 Team Organization

Our CiiMAV team consists of 16 members which comprise of current students of Aerospace Engineering (AE) and International Double Degree Program of Aerospace Engineering (IDDP). Each member in our team has different interests and capabilities make our team even more perfect. In addition, our team has been advised and supported by advisor. This flowchart illustrates the team's organization.

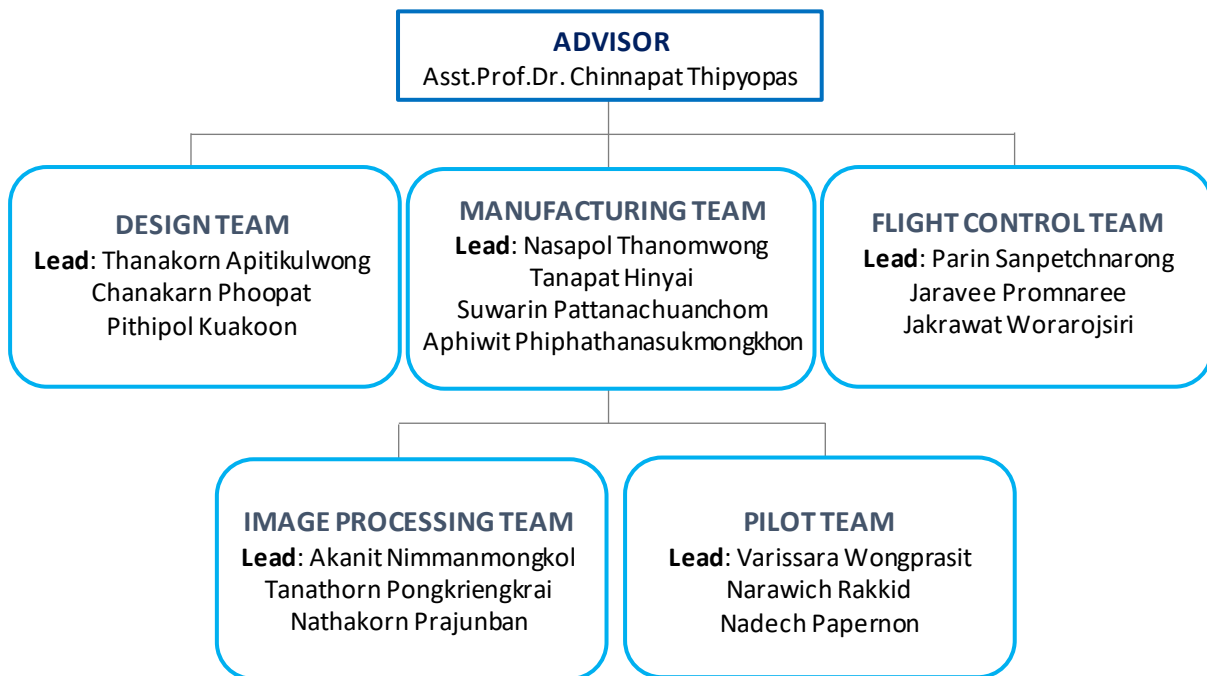


Figure 2 : Team Organization

From the flowchart, the members will be divided into five sub-teams according to their interests. Sub-team will have a different responsibility to be able to work efficiently.

- **Design Team:** After our CiiMAV team had concluded our UAV conceptual design. Preliminary and detailed design tasks will be conducted by the design team. The design team is also responsible for 3D CAD model of the UAV.
- **Manufacturing Team:** After final design of the UAV has been completed, manufacturing team will start manufacturing process to fabricate the UAV according to the design. Which includes the use of CNC machine and hot-wire foam cutting apparatus. Moreover, manufacturing team will also be heavily involved in composite material, which will be extensively used in fuselage construction.
- **Flight Control Team:** This team is responsible for autopilot systems including flight path planning, GPS, and antenna trackers so that our UAV can complete the missions safely in the competition.
- **Image Processing Team:** This team is responsible for the design of the imagery system and its layout according to the mission objectives.



- **Pilot Team:** Responsible for tuning of flight control surfaces and command the aircraft throughout the entire mission. The team must ensure that there will be no harm to participants and no damage upon the UAV.

## 2.1 Project Milestone Chart

Milestones of all relevant processes are illustrated by using a Gantt chart to visualize schedule for design and fabrication of the UAV. Our team will work through this plan to ensure that all UAV systems will be fully prepared for the upcoming competition.

MILESTONE	JUNE	JULY	AUG	SEP	OCT	NOV	DEC	JAN
<b>UAV Design</b>								
Conceptual Design	■							
Preliminary	■							
Detailed Design	■■■							
CAD Model	■■■■							
<b>Manufacturing</b>								
UAV Components		■■■■■						
Payload System			■■					
Camera Part			■■					
Electronic Part			■■					
<b>Flight Control</b>								
Auto pilot		■■■■■						
Antenna Tracker		■■■■■						
System testing			■■■■■					
<b>Image Processing</b>								
System Design		■■■■■						
System Testing			■■■■■					
<b>UAV Testing</b>								
Structure		■■■■■						
Propulsion			■■■■■					
Full System Testing				■■■■■				
<b>First Flight</b>				■■■■■				
<b>Mission Practice</b>					■■■■■			
<b>AAVC Competition</b>								■■■■■

Table 1 : Project Milestone

## 3.0 Conceptual Development

According to the mission requirements (Surveillance and Reconnaissance operation), the conceptual design phase was initiated based on configurations commonly used in such missions. The initial configuration and sizing of the hybrid UAV will be selected based on the results of the analysis, in which configuration with the highest scores will ultimately be chosen for the mission. Score criterion will be created by referring to the mission objectives.

### 3.1 Mission Requirement

Based on published rules and restriction of AAVC 2021-2022 competition, which imposed no limits on UAV platform configurations. The primary concept of hybrid UAV design is to optimize between drag, lift, weight, thrust, and structural strength. While being able to operate with limited take-off and landing zones.

#### 3.1.1 Hybrid Mission Requirements and Concerns

- Maximum assembly time of 5 minutes.
- Safety take-off and Landing operations within specified mission zones.
- Identify the exact location (GPS coordinate) of all targets.
- Identify the details and overall shape of a specific target.
- Payload drop accuracy (on one of the targets).
- Loiter flight over target area and maintain target in image frame for 60 seconds.
- Operating the mission in 15 minutes and no damage to the UAV.

<b>Payload weight</b>	0.5 – 1 kg
<b>Payload shape</b>	A cylindrical bottle (Diameter ≈ 65 mm, length ≈ 240 mm)
<b>Search area (fixed wing/hybrid)</b>	1100 x 700 m
<b>Launching pad area</b>	5 x 5 m
<b>Endurance</b>	15 min

Table 2 : Requirement

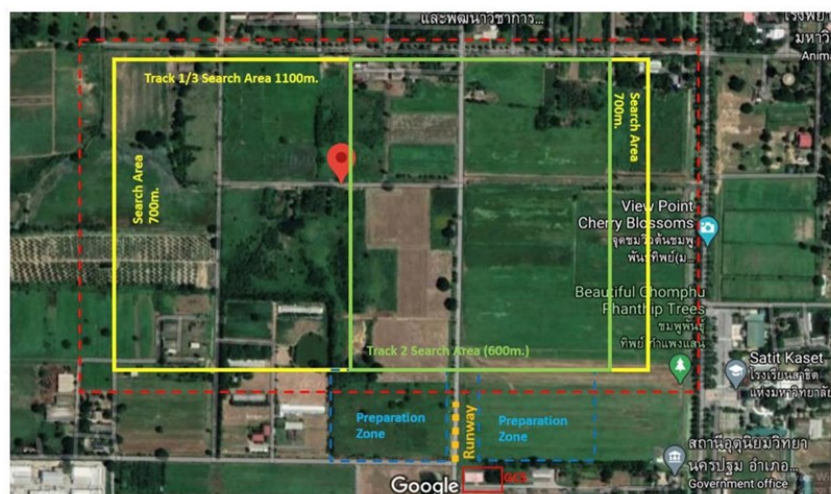


Figure 3 : Overview of Operating Area

### 3.1.2 Hybrid Total Mission Score

No.	Criteria	Equation	Maximum Score	Remark
1	Safely take-off	-	10	
2	Payload drop accuracy	$P_{acc,drp} = [2(15 - D)] + (20/n)$	50	D = distance from the target (m) n = number of drop trials
3	Loitering time over each target	$P_{loit} = 0.5t$	60	t = total time that the target stays in image frame (max = 60 sec) [max point per target = 30]
4	Target identification	Overall shape of the target	10	
		Details on the target	10	
5	Target location accuracy	$P_{GPS} = 20(f_{acc,GPS})$	20	$f_{acc,GPS}$ = accuracy factor (Error within 5 m radially from target gets 20 points, while error exceed 50 m radially gets 0 point)
6	Landing location accuracy	-	10	Landing within the perimeter of the launchpad gets 10 points.
7	Condition after landing	-	20	Landing with no damage gets 20 points.
8	If use operation time exceeded 15 minutes, every one minute that exceed will results in "-5" penalty to total score.			

Table 3 : Mission Score

Furthermore, there are two multiplication factors:

- **Autonomy level factor ( $f_{auto}$ ):** the system's level of autonomy

Level of autonomy	Factor	Description
High	1.5	Manual control
Medium	1.25	Automatic flight, the UAV does not decide by itself
Low	1	On board decision, no interference by ground staff

Table 4 : Autonomy Level Factor

- **Payload capacity factor ( $f_{ply}$ ):** the vehicle's weight efficiency

-  $RP$  is the fraction of payload weight and take-off weight of each team.

$$RP = \left( \frac{W_{payload}}{W_{to}} \right)$$

- $F_p$  is the fraction of payload weight ratio of each team and maximum payload weight ratio team with the highest RP.

$$F_p = \left( \frac{PR_i}{PR_{max}} \right)$$

Total mission score

$$\text{Mission Score} = f_{\text{ply}} \times [f_{\text{auto}} \times (\text{No. 1} + \text{No. 2} + \text{No. 3} + \text{No. 4} + \text{No. 5} + \text{No. 6} + \text{No. 7})]$$

### 3.2 Sensitivities Matrix

#### SCORE RATIO FOR HYBRID UAV

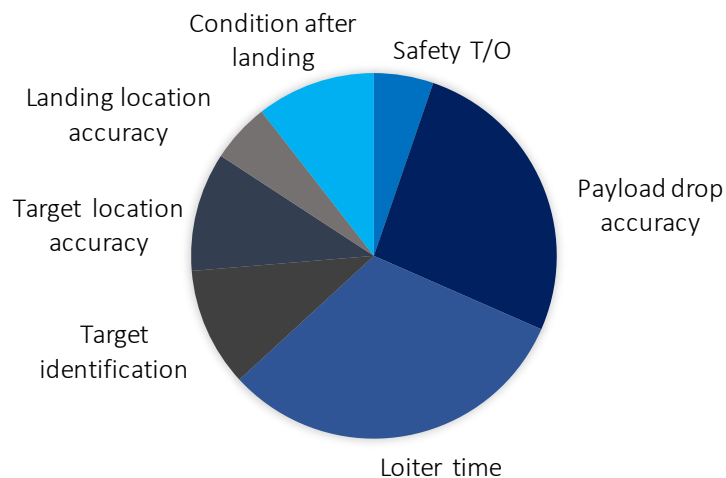


Figure 4 : Score Ratio

From total mission score equation and score composition illustrated above, the critical parameters that had major effect on total mission score are autonomy level factor, vehicle's weight efficiency, payload drop accuracy, loiter time score and target location accuracy.

As a result, the crucial ideas for design UAV were obtained from sensitivity analysis. Key design traits of the UAV are low drag, high lift force, lightweight, accurate and reliable drop mechanism, and has high resolution image for highest mission score.

### 3.3 Converting Mission Requirements into Design Requirements

From mission requirements and sensitivities analysis, yields a conceptual design of the UAV that must be able to complete the mission within 15 minutes. The UAV needs to possess low drag, which results in less power required. Subsequently, results in a smaller battery and motor. Moreover, the design must have high lift force to accommodate heavier payload while maintaining a lightweight structure. Furthermore, the design must not compromise structural strength.

Task	Solution
Preparation time before flight is 5 mins.	The UAV should have minimal complexity for minimal system set up and able to be assemble within 5 mins.
A launchpad is 5x5 m	To achieve vertical flight capability, key component to consider is the aircraft's vertical flight motor(s) output must be equal or more than aircraft weight. This depends on the desired degree of maneuverability during vertical flight phase.
Safely take-off and landing with no damage	<ul style="list-style-type: none"> <li>- The structure design must have sufficient strength.</li> <li>- The landing gear and fuselage design need to be sturdy enough to withstand shock loads generated during landing.</li> </ul>
Identify the exact location (GPS coordinate) of target, overall shapes, and details of the target	<ul style="list-style-type: none"> <li>- The image processor has suitable capabilities for target detection and tracking.</li> <li>- The image system with high resolution and reliable data transmission system.</li> <li>- The camera should have suitable resolution for UAV cruise altitude.</li> <li>- Plan search path for target acquisition.</li> </ul>
An aircraft shall have the payload handling system and release the payload at specific target in the mid-flight.	<ul style="list-style-type: none"> <li>- For maximum payload weight, the UAV should have high lift and the payload bay needs to be arrange such that the fuselage produce minimum drag.</li> <li>- The UAV has a robust, light, and accurate drop mechanism.</li> </ul>
Loiter flight over target area and maintain image frame for 60 seconds.	Identify the target and loitering over the target with an optimized turning radius.
Operating the mission in 15 minutes	Design the UAV with high performance to accomplish the mission within time constrain.

Table 5 : Mission Requirements and Solution

### 3.4 Conceptual Design Selection

In this section, each component will be evaluated by using scoring process or trade-off study to determine the most practicable options for the mission requirements. Also, the criteria for configuration selection for each part and their weight scores are provided with description below.

### 3.4.1 UAV Configuration Selection

Criterion below is used to score the aircraft configuration concepts.

- **Low structural weight (50%):** From the requirements, the weight of the aircraft is one of the most critical components and is also used for mission score multiplier. All in all, to achieve highest score the structural weight must be as low as possible.
- **Stability (35%):** The advantages of high stability design is resilience to disturbance, thus, better hand-off flying quality.
- **Ease of Manufacturing (15%):** The advantages of a simple to build design is reduction of time and cost. Simple parts are easier to rebuild or fix in case of damage.

#### Configuration Selection

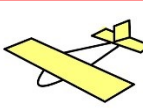
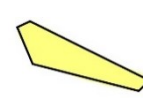
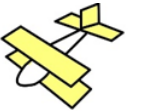
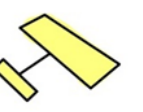
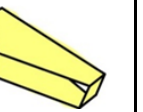
						
Criteria	Weight	Conventional	Flying Wing	Biplane	Canard	Double Flying Wing
Low structural weight	50%	3	5	2	4	2
Stability	35%	4	1	4	2	3
Ease of Manufacturing	15%	3	2	2	3	1
Total	100	3.35	3.15	2.7	3.2	2.2

Table 6 : Aircraft Configuration Selection

From the table above, conventional configuration was selected which allows for more flexibility to modify the design. The design is also the most simple and easy to build.

### 3.4.2 Wing location Configuration Selection

Advantages of each wing location listed below were used to determine the wing vertical location configuration.

- **High wing:** For high wing, the wing of an aircraft is located on the upper fuselage section. It is considered as the most stable and increase roll stability. This design also has the least influence from ground effect when compared to others configuration.
- **Mid wing:** For mid-wing, the wing of an aircraft is located approximately halfway up the fuselage. It has light weight and easy to manufacture. Mid wing design also possess the least interference drag of all configurations.
- **Low wing:** For low wing, the wing of an aircraft is located at the bottom of the fuselage. This design has greatest influence from ground effect but is the least stable when compared to other configurations.

				
Criteria	Weight	High wing	Mid-wing	Low wing
Control	40%	4	3	2
Lightweight	30%	3	5	3
Interference	30%	3	5	2
<b>Total</b>	<b>100</b>	<b>3.4</b>	<b>4.2</b>	<b>2.3</b>

Table 7 : Wing Location Configuration Selection

From mission requirements, the selected conceptual configuration is mid-wing which has light weight, easy to build, and lowest drag of all configurations.

### 3.4.3 Landing Gear Configuration Selection

The criterion below is used to score the landing gear configurations.

- **Clearance (45%):** To achieve take-off distance within 100 meters. The UAV must have enough thrust required for take-off with carried payload. Thus, it should have enough clearance for propeller length. Moreover, the design must provide clearance when the aircraft is converted into a vertical take-off and landing variant.
- **Strength (35%):** For safely taking-off and landing with no damage. The landing gear design needs to be sturdy enough to withstand the forces generated during take-off and landing.
- **Weight (20%):** From mission requirements, the weight of the UAV is one of the most important criteria in total mission scoring. Thus, the component must be as light as possible to get higher score.

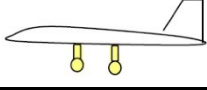
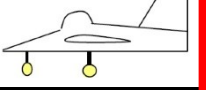
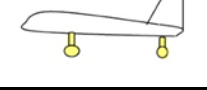
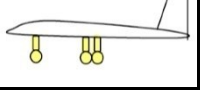
					
Criteria	Weight	Bicycle	Tricycle	Taildragger	Multi-gear
Clearance	45%	3	4	2	2
Strength	35%	2	3	3	3
Weight	20%	4	3	3	1
<b>Total</b>	<b>100</b>	<b>2.85</b>	<b>3.45</b>	<b>2.55</b>	<b>2.15</b>

Table 8 : Landing Gear Configuration Selection

The selected landing gear configuration is a tricycle which has enough propeller clearance for both conventional and vertical take-off and landing variant, possess strong structure and lightweight construction.

### 3.4.4 Propeller Configuration and Location Selection

Criterion below is used for scoring the propulsion system placement concepts.

- **System Weight (50%):** From mission requirements, the weight of the UAV is one of the most important criteria in total mission scoring. The design must possess lowest weight

as possible to achieve highest score. More number of motors will result in a higher weight.

- **Power (30%):** The power output from the system will be proportional to the number of motors fitted to the aircraft. With two motor concepts will deliver greater overall power (thus, has higher score than single motor configuration).
- **Power consumption (20%):** Endurance of an aircraft is affected by motor power consumption and from aerodynamic drag of the aircraft. The UAV must complete the mission within 15 minutes, greater flight speed comes with greater aerodynamic drag.

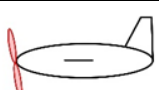
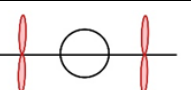
					
Criteria	Weight	Single Tractor	Single Pusher	Twin Motor	Tractor-Pusher
System Weight	50%	3	4	1	1
Power	30%	3	3	5	5
Power consumption	20%	3	3	1	1
Total	100	3	3.5	2.2	2.2

Table 9 : Propeller Configuration and Location Selection

Since, we wanted to design the UAV that can converted into both fixed-wing and hybrid UAV variants. With less obstruction to the imagery system, optimal power consumption, and optimal power output. Thus, the most suitable propeller configuration for our requirement is single pusher.

### 3.4.5 Tail Configuration

Advantages listed below is used to evaluate empennage configuration of the aircraft.

- **Conventional tail:** The conventional tail provides optimal stability and control, with the most optimal structural weight. However, the horizontal stabilizer was affected by a downwash of the wing. Furthermore, with rear powerplant placement, cause more stress on the propeller as it travels through different pressure gradients of the empennage airfoil on every rotation. Moreover, this tail configuration will cause complications when the aircraft was reconfigured to a vertical take-off and landing variant; therefore, this configuration is deemed unsuitable.
- **V-tail:** The V-tail is generally lighter and have less surface area needed compared to the conventional tail (it has dual purpose control surface) and with less protrusion leads to drag reduction. However, this configuration possesses similar problems as the conventional tail configuration. Reconfiguration to a vertical flight capable variant would demerit the weight benefit of this empennage arrangement.
- **T-tail:** T-tail arrangement possesses better aerodynamics due to the horizontal stabilizer is located away from turbulent airflow from other components. Besides, T-tail is heavier than the conventional tail due to requirement of the reinforced vertical tailplane. Additionally, T-tail designs are susceptible to unrecoverable deep-stall

conditions if the aircraft reach certain pitch angle. Despite being aerodynamic, the arrangement did not facilitate conversion to a vertical flight capable variant and will results in an increase in structural mass of the aircraft.

- **H-tail:** H-tail arrangement benefits from endplate effect of the horizontal stabilizer. The H-tail is generally heavier than the conventional tail because the horizontal tail must be reinforced to support both vertical tails. Consequently, due to more effective tailplane, the stress on the rear mounted propeller would be greater. Additionally, with greater effect on weight, the configuration possesses more difficulties to convert to a vertical flight capable variant.
- **Inverted-U tail:** Despite higher drag than that of the conventional tail arrangement. The inverted U-tail with twin boom construction is more suitable for the rear powerplant placement. Moreover, the efficiency of the horizontal tailplane will be increased due to the tailplane being situated above the propwash regime. Twin boom construction enhances the stiffness of the tail and stops it from twisting. Furthermore, twin boom structure greatly benefits the conversion into a vertical take-off and landing variant. As the vertical lift motors and relevant extensions can easily be reconfigured for such configuration.

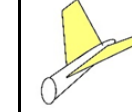
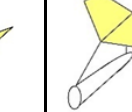
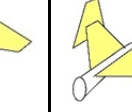
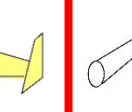
						
Criteria	Weight	Conventional	V-tail	T-tail	H-tail	Inverted U
Control	40%	2	1	2	5	5
Weight	30%	4	5	3	1	2
Drag	20%	3	4	3	3	3
Structure	10%	3	2	3	3	3
Total	100	2.9	2.9	2.6	3.2	3.3

Table 10 : Tail Configuration Selection

The selected configuration for empennage design is a twin boom inverted U-tail. Since, we wanted to design the UAV that can easily be converted into both fixed-wing UAV and hybrid UAV. Moreover, our propeller configuration is a single pusher, extra protection to the propeller from the twin boom assembly proved that this design met most of our requirements.

In conclusion, the selected conceptual design configuration of every component reflects the designed requirements for maximum mission score and aircraft modularity capable of converting into both fixed-wing and VTOL variant. Therefore, our conceptual design is a mid-wing monoplane with twin boom inverted U-tail empennage, powered single pusher propulsion and supported by a tricycle landing gear configuration.

### 3.5 Planform parameter

#### 3.5.1 Wing Sizing

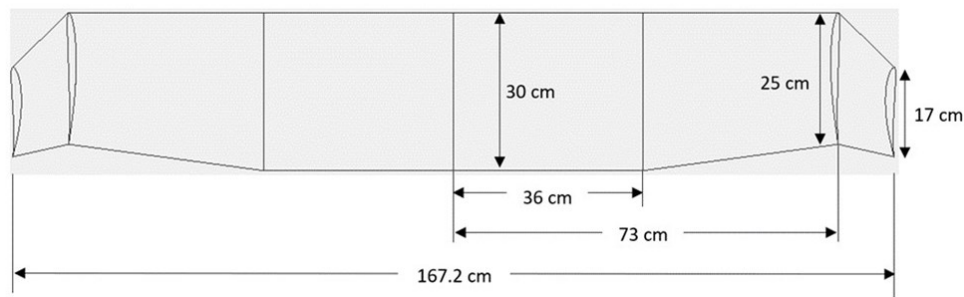


Figure 5 : Wing Dimension (Top View)

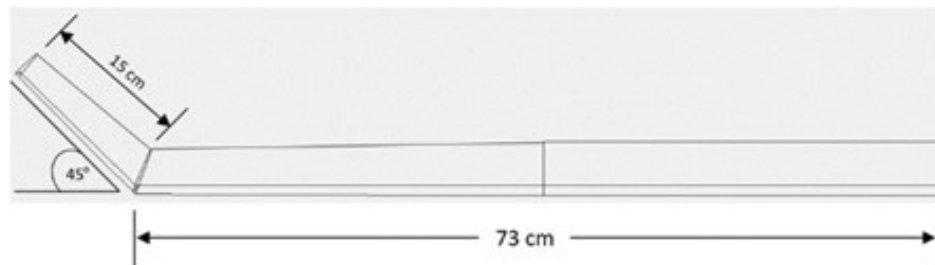


Figure 6 : Wing Dimension (Front View)

<b>Airfoil</b>	MH 113
<b>Span</b>	176 m
<b>Project span</b>	167.2 cm
<b>Root chord</b>	30 cm
<b>Mid chord</b>	25 cm
<b>Tip chord</b>	17 cm
<b>Mean chord</b>	27.8 cm
<b>Wing area</b>	48 cm <sup>2</sup>
<b>Project wing area</b>	46 cm <sup>2</sup>
<b>Aspect ratio</b>	6.42
<b>Taper ratio</b>	0.568
<b>Dihedral</b>	45°
<b>Sweep angle</b>	4.39°
<b>Incident angle</b>	2°

Table 11 : Wing Configuration

### 3.5.2 Horizontal Tail Sizing

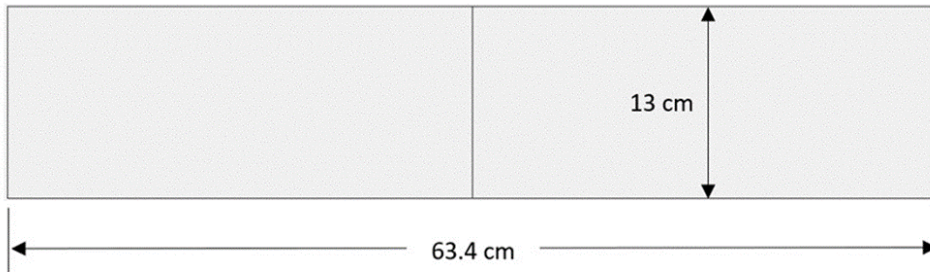


Figure 7 : Horizontal Tail Dimension (Top View)

<b>Airfoil</b>	NACA 0012
<b>Span</b>	63.4 m
<b>Root chord</b>	13 cm
<b>Tip chord</b>	13 cm
<b>Mean chord</b>	13 cm
<b>Wing area</b>	8 cm <sup>2</sup>
<b>Aspect ratio</b>	4.88
<b>Taper ratio</b>	1
<b>Sweep angle</b>	0°
<b>Incident angle</b>	0°

Table 12 : Horizontal Tail Configuration

### 3.5.3 Vertical Tail Sizing

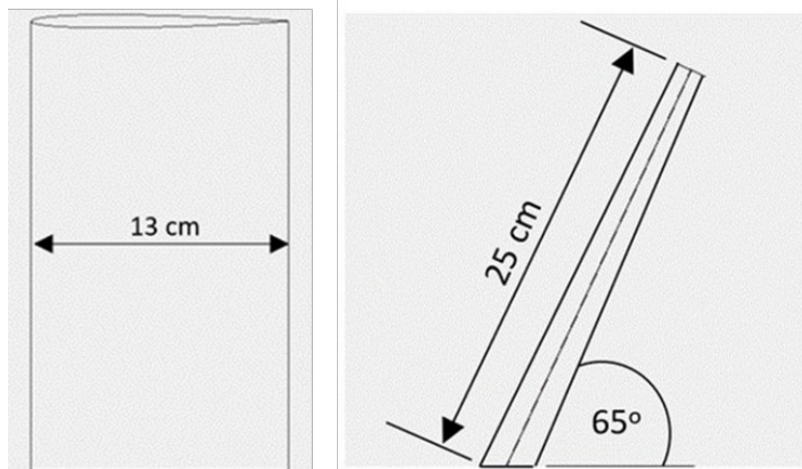


Figure 8 : Vertical Tail Dimension



Airfoil	NACA 0012
Span	25 cm
Project span	22.5 cm
Root chord	13 cm
Tip chord	13 cm
Mean chord	13 cm
Wing area	7 cm <sup>2</sup>
Project Wing area	6 cm <sup>2</sup>
Aspect ratio	3.85
Taper ratio	1
Dihedral	65°
Sweep angle	0°
Incident angle	0°

Table 13 : Vertical Tail Configuration

### 3.6 Drag Estimation

From fix-wing

Assume skin friction drag coefficients of landing gear

Find skin friction drag coefficient of wing and tail

$$C_D = C_{D_0} + K C_L^2$$

$$C_{D_{wing-tail}} = C_{D_{0wing-tail}} + \frac{1}{\pi \cdot e \cdot AR} C_L^2$$

$$0.064 = C_{D_{0wing-tail}} + \frac{1}{\pi \times 0.8 \times 6.42} \cdot 0.93^2$$

$$C_{D_{0wing-tail}} = 0.0104$$

Find skin friction drag coefficient of fuselage from CFD  $C_{D_{0fuselage}} = 0.0066$

$$C_{D_{0fuselage}} = C_{D_{fuselage}} \left( \frac{S_{fuselage}}{S_{wing}} \right) = 0.0066 \times \left( \frac{0.018}{0.464} \right) = 0.000256$$

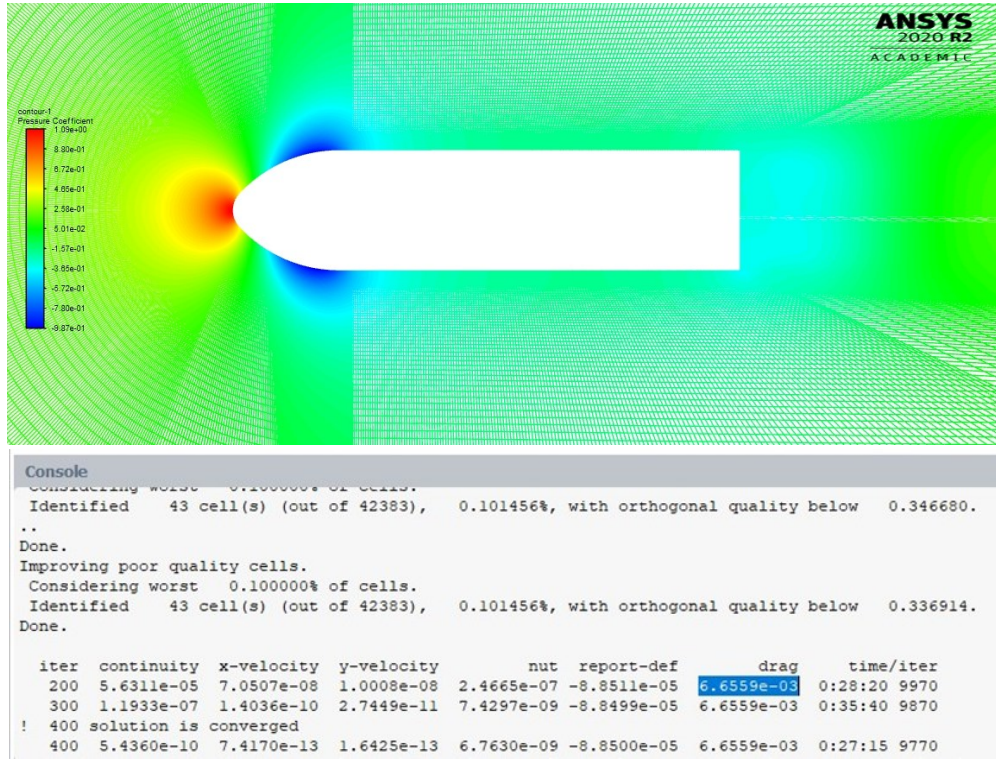


Figure 9 : CFD Analysis

Despite the aircraft was designed with modularity in mind, there exist some changes to the exterior geometry of the aircraft that cannot be neglected. Protrusion of some components, notably the 4 motors used for its vertical take-off and landing capabilities, caused deviation from what was simulated on XFLR5 program. Thus, drag estimation on the design must be done for future references and calculation of the aircraft overall performance. Approximation was calculated by utilizing wetted cross section area of the component when the aircraft is in level flight. The dimensions were based on the mechanical drawings of the components readily available on the internet.

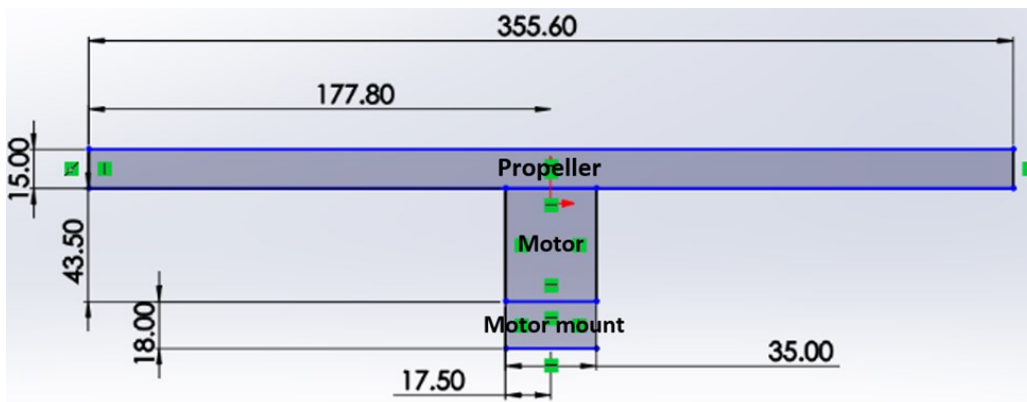


Figure 10 : Approximated Wetted of Motor Assembly, Front View (Unit mm)

			$C_L$	$C_D$
Circular place		→	0	1.17
Circular cylinder	L/D 0.5	→	0	1.15
	1	→		0.90
	2	→		0.85
	4	→		0.87
Rectangular plate	L/D	→	0	1.18
Rectangular cylinder	1	→	0	1.20
	5	→		1.30
	10	→		1.50
	20	→		1.98

Figure 11 : Drag Coefficient for Other Shape

Interpolation yields:

$$C_{D_{motor}} = 0.998$$

$$C_{D_{prop}} = 0.673$$

$$C_{D_{mount}} = 1.225$$

Find skin friction drag coefficients of quad plane.

$$C_{D_{0,motor}} = \sum_{i=1}^4 C_{D_{motor}} \left( \frac{S_{motor}}{S_{wing}} \right) = 4 \times 0.998 \times \left( \frac{(43.5 \times 10^{-3})(35 \times 10^{-3})}{0.464} \right) = 0.013$$

$$C_{D_{0,prop}} = \sum_{i=1}^4 C_{D_{prop}} \left( \frac{S_{prop}}{S_{wing}} \right) = 4 \times 0.673 \times \left( \frac{(15 \times 10^{-3})(355.6 \times 10^{-3})}{0.464} \right) = 0.031$$

$$C_{D_{0,mount}} = \sum_{i=1}^4 C_{D_{mount}} \left( \frac{S_{mount}}{S_{wing}} \right) = 4 \times 1.2 \times \left( \frac{(18 \times 10^{-3})(35 \times 10^{-3})}{0.464} \right) = 0.0067$$

$$\begin{aligned} C_{D_{0,quadplane}} &= K_c \left[ C_{D_{0,wing-tail}} + C_{D_{0,fuselage}} + C_{D_{0,LDG}} + C_{D_{0,motor}} + C_{D_{0,prop}} + C_{D_{0,mount}} \right] \\ &= 1.2 [0.0104 + 0.000256 + 0.012 + 0.013 + 0.031 + 0.0067] = 0.088 \end{aligned}$$

Find drag coefficient of quad plane.

$$C_D = C_{D_0} + \frac{1}{\pi \cdot e \cdot AR} C_L^2$$

$$C_{D_{quadplane}} = C_{D_{0,quadplane}} + \frac{1}{\pi \cdot e \cdot AR} C_L^2$$

$$C_{D_{quadplane}} = 0.088 + \frac{1}{\pi \times 0.8 \times 6.42} \cdot 0.93^2 = 0.1416$$

Initially, aircraft weight estimation is based on previous UAV design by CiiMAV team. In this mission, we approximated the structural weight to be within 4 kg and capable of handling maximum payload weight for 1 kg.

To generate a matching plot diagram, we substitute value of  $C_{D_0}$  from drag estimation calculations to every related function to determine wing sizing and motor selection. The matching chart for propeller aircraft is generated by plotting power loading versus wing loading of the aircraft. Power loading is the weight of the aircraft divided by the output power of the powerplant. Whereas the wing loading is the weight of the aircraft over the wing area of the aircraft

Our design will be affected by 5 factors. First, the stall speed, which is calculated by equation 1. Stall speed relates to the wing area of the aircraft, to achieve level flight the aircraft must have optimal wing area to its operational weight. The stall speed criterion is displayed by the green line in the plot below. The acceptable design points for this criterion are located to the left of the plot. Next, the cruise speed is considered. Cruise speed is computed by maximum power and efficiency of propeller. The relation of aircraft wing loading to aircraft cruise speed is shown in equation 2 and plotted in orange line in the graph below. Acceptable design region is located below the curve plot.

Furthermore, the relation of aircraft power loading to aircraft rate of climb criterion is represented by equation 3. The function is represented by yellow line on the matching plot, respectively, the acceptable design region is located below the curve. Whereas the relation to take off distance criterion can be computed by equation 4. This function is represented on the plot with a blue line. The acceptable design region is located below the blue curve. Eventually, the aircraft ceiling is governed by the aircraft's rate of climb at a certain altitude and is defined by equation 5. The relation is plotted with a grey line. Region of acceptable design points is located below the relation curve.

$$\left(\frac{W}{S}\right)_{V_s} = \frac{1}{2} \rho V_s^2 C_{L_{max}} \quad (1)$$

$$\left(\frac{W}{S}\right)_{V_{cruise}} = \frac{\eta_p}{\frac{1}{2} \rho V_{cruise}^3 C_{D_0} + \frac{2K}{\rho \sigma V_{cruise}} \left(\frac{W}{S}\right)} \quad (2)$$

$$\left(\frac{W}{P}\right)_{ROC} = \frac{1}{\frac{ROC}{\eta_p} + \sqrt{\frac{2}{\rho \sqrt{\frac{3C_{D_0}}{K}}} \left(\frac{W}{S}\right) \left(\frac{1.155}{(\frac{L}{D})_{max} \eta_p}\right)}} \quad (3)$$

$$\left(\frac{W}{P}\right)_{T/O} = \frac{1 - \exp(0.6 \rho g C_{D_G} S_{TO} \frac{1}{W/S})}{\mu - \left(\mu + \frac{C_{D_G}}{C_{L_R}}\right) \left[\exp(0.6 \rho g C_{D_G} S_{TO} \frac{1}{W/S})\right]} \eta_p \quad (4)$$

$$\left(\frac{W}{P_{SL}}\right)_C = \frac{\sigma_{AC}}{\frac{ROC_C}{\eta_p} + \sqrt{\frac{2}{\rho \sigma_{AC} \sqrt{\frac{3C_{D_0}}{K}}} \left(\frac{W}{S}\right) \left(\frac{1.155}{(\frac{L}{D})_{max} \eta_p}\right)}} \quad (5)$$

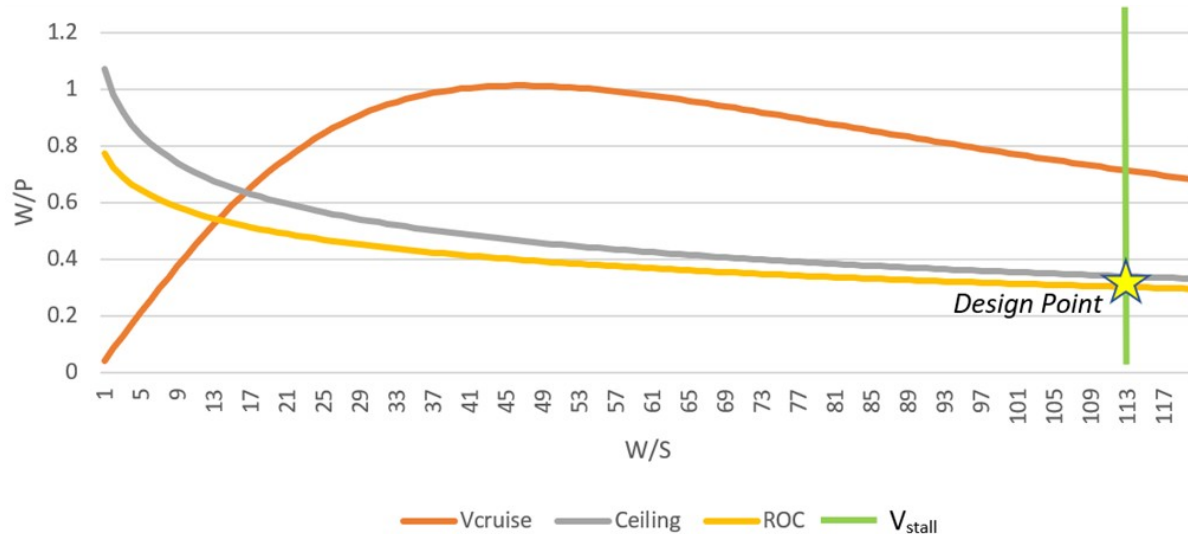


Figure 12 : Matching Chart

According to matching chart of power loading (W/P) and wing loading (W/S) graph above, the envelope to operate the fixed-wing UAV is in the overlap region that below the four lines and to the left of the stall speed function. Thus, the selected design point (represented by the star) is an intersection between  $V_{stall}$  line and ROC line. Which the point that has ROC with 150 ft/min and designed stall velocity of (10.43 m/s). With parameters taken from the design point represents the most optimal value of wing and power loadings. Thus, the optimal motor size and optimized wing area were ultimately defined.

From selected design point, the power loading (W/P) is 0.3 and the wing loading (W/S) is 113. If the maximum take-off load is defined as 5 kg, the power required should be around 166.67 watts and the wing area required should be 0.442 m<sup>2</sup>.

### 3.7 Motor and Battery Selection

The motor is one of the most crucial components of an airplane since it generates the thrust that allows the airplane to fly. Primarily, brushless DC motors were more preferable based on past design experience. Brushless DC motors also provide the advantages of very accurate speed control, great efficiency, and reliability.

First, for motor selection of propeller aircraft. Using a steady level flight conditions where primary forces on an aircraft during steady flight are illustrated in the figure below. While our designed maximum takeoff weight of quad plane is 5 kg and has (L/D) ratio of 14.468, obtained from XFLR5 program.

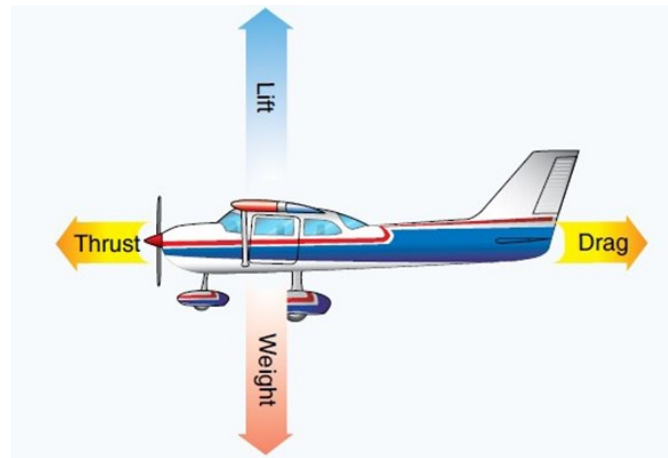


Figure 13 : Force on Aircraft in Level flight

Thus, the relation between force equilibrium is given by

$$Thrust = Drag \quad (1)$$

$$Lift = Load\ Factor \times Weight \quad (2)$$

$$(1)/(2) ; \frac{Thrust}{Weight \times Load\ Factor} = \frac{Drag}{Lift} = \frac{1}{\frac{Lift}{Drag}} = \frac{1}{14.468} = 0.07$$

Therefore, thrust required is calculate by

$$\begin{aligned} Thrust &= 0.07 \times Weight \times Load\ Factor \\ &= 0.07 \times 5000 \times 2.5 = 875\ g \end{aligned}$$

From calculation above, the minimum thrust required must be at least 875 g and the power required should be around 166.67 watts. As a result, we decided to use SunnySky X3520 Brushless Motors KV720 which has a thrust force of 1250 g, a power of 177.60 watts and APC13\*8 propeller for horizontal flight phases (for cruising).

Prop (inch)	Voltage (V)	Amps (A)	Thrust (gf)	Watts (W)	Efficiency (g/W)
APC13*8	14.8	3.6	500	53.28	9.38
		6.1	750	90.28	8.31
		8.9	1000	131.72	7.59
		12	1250	177.60	7.04
		15.7	1500	232.36	6.46

Table 14 : Motor Specification

According to the calculation above, the minimum lift force required must be at least 5000 g. Therefore, we decided to use 4 pieces of EMAX multi-copter motor MT3515 650 KV which has a thrust rating of 1450 g, a power of 266.40 watts and Carbon Fiber 12\*3.8 propellers for vertical flight phases (for loiter).

Prop (inch)	Voltage (V)	Amps (A)	Thrust (gf)	Watts (W)	Efficiency (g/W)
Carbon Fiber 12*3.8	22.2	10	1300	222.0	5.9
		12	1450	266.4	5.4
		14	1640	310.8	5.3
		16	1780	355.2	5.0
		18	1920	399.6	4.8

Table 15 : VTOL Motor Specification

Additionally, for this competition a battery with lightweight, high capacity, and high discharge rate is preferred. Thus, we decided to use a Lithium-Polymer (Li-Po) battery from the requirements. Moreover, the voltage supplied by the battery must be at least equal to the voltage of the motor to operate. Which is 22.2 volt for this requirement.

Here, we must accomplish the mission within 15 minutes and the motor requires 12 amps of electric current, according to the mission requirements. In conclusion, we may use the equation below to calculate the battery capacity.

$$\begin{aligned}
 \text{Battery Capacity} & [Amps/hour] \\
 &= [\text{Quantity of Motors [pieces]} \times \text{Current [Amps]} \\
 &\quad \times \text{Flight Time [hour]}]_{\text{loiter}} \\
 &\quad + [\text{Current [Amps]} \times \text{Flight Time [hour]}]_{\text{forward}} \\
 &= [4 \text{ pieces} \times 12 \text{ Amps} \times \frac{15 \text{ min}}{60 \text{ min}}]_{\text{loiter}} + [12 \text{ Amps} \times \frac{15 \text{ min}}{60 \text{ min}}]_{\text{forward}} = 15000 \text{ mAh}
 \end{aligned}$$

Calculation above yields desired battery capacity of 15000 mAh. Thus, we selected 16000 mAh battery as shown in figure below.



Figure 14 : Baterry 16000 mAh

## 4.0 Preliminary and Detailed design

### 4.1 Aerodynamic Analysis

Aerodynamics group is responsible for the design optimization and drag reduction of the aircraft. Iterative process was used to determine geometric parameters of aerodynamic components and ensures smooth integration to other aircraft components. The process starts with selection of airfoils for aerodynamics surfaces, for instance wings and empennage. 3D performance characteristics were evaluated and verified with the design requirements. Aerodynamics group is also responsible for evaluating preliminary testing data obtained from Computational Aerodynamics software XFLR5.

#### 4.1.1 Aerodynamics prediction

The aerodynamics performance is evaluated at Reynolds number range of 50,000-700,000 as per predicted stall and cruise velocities.

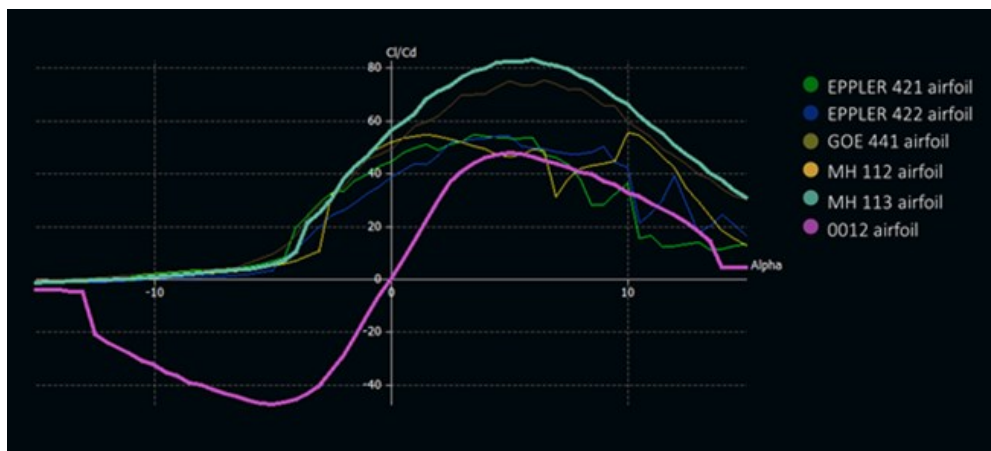


Figure 15 :  $Cl/Cd$  VS  $\alpha$

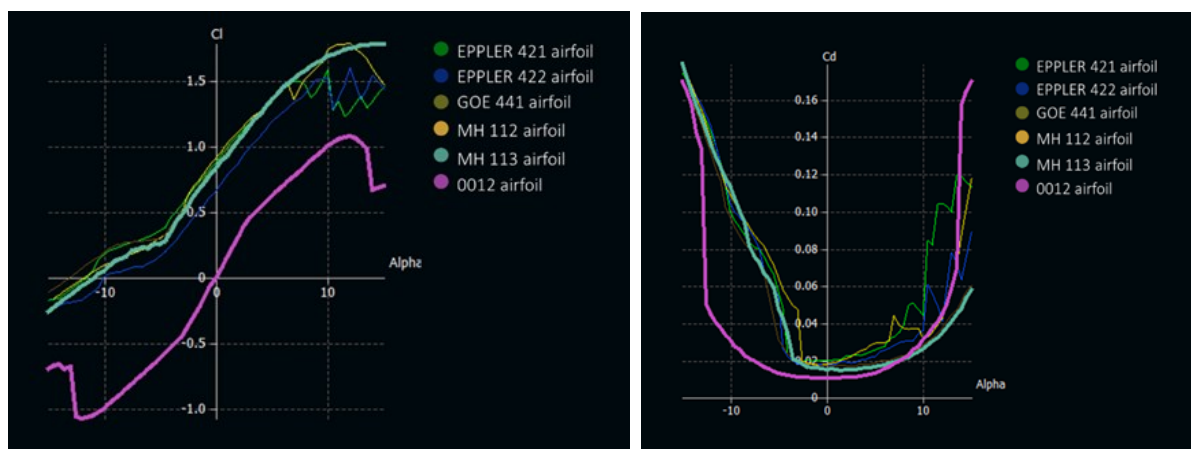


Figure 16 :  $Cl$  VS  $\alpha$  and  $Cd$  VS  $\alpha$

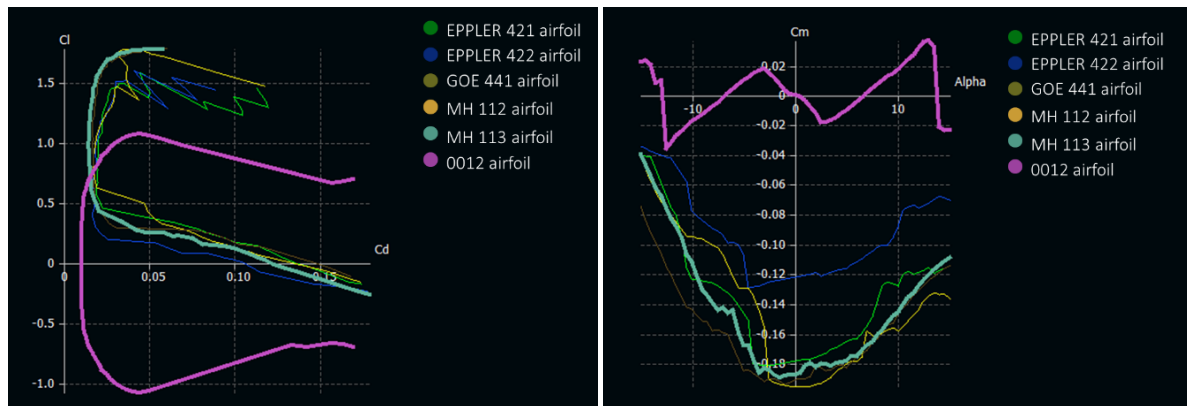


Figure 17 :  $C_l$  VS  $C_d$  and  $C_m$  VS  $\alpha$

#### 4.1.2 Airfoil Selection



Figure 18 : 0012 Airfoil



Figure 19 : MH 113 Airfoil

A preliminary survey on “High Lift Low Reynolds number” airfoils was conducted. Several airfoils were disregarded from maximum lift coefficient and manufacturability constrains. The airfoil needs to possess sufficient thickness to accommodate structural components of the aircraft and feasible for hot-wire cutting, while optimizing drag at different speeds. After completing airfoil analysis using XFLR5 program, airfoil MH113 was ultimately selected due to high lift and high lift-to-drag ratio while also possessing sufficient thickness suitable for subsequent manufacturing. For the empennage section the airfoil NACA 0012 was chosen due to compatible airfoil thickness.

### 4.3 Structural Analysis

Wing is a crucial component that produce lifting force for the aircraft. To maintain level flight, the wings must be able to support gross weight of every component of the aircraft. The structure can be idealized as a cantilevered beam (considering half of the aircraft, due to symmetry). One of major challenges of structural design of the wing involves a light-weight design that is strong enough to accommodate stress that occur during flight.

Structure analysis is done based on data from preliminary design process.

<b>Airfoil</b>	MH 113
<b>Thickness</b>	14.7% @ 29.7% Chord
<b>Camber</b>	6.4% @ 47.7% Chord
<b>Wingspan [m]</b>	1.76
<b>Root Chord [m]</b>	0.3
<b>Tip Chord [m]</b>	0.17

Table 16 : UAV Configuration



Figure 20 : MH 113 Airrfoil

Using XFLR5 program for 3D analysis, lift coefficient vs. Span plot can be produced.



Figure 21 : Lift Coefficient VS Span Plot

### 4.3.1 Aero Lift

Using Microsoft Excel program for change local lift coefficient to load on wing. Call that “Aero lift”.

$$L = \frac{1}{2} \rho v^2 S C_l$$

Where      L      =      Aero lift [N]  
 $\rho$       =      Density [kg/m<sup>3</sup>]  
 $v$       =      Velocity [m/s]  
S      =      Wing area [m<sup>2</sup>]  
 $C_l$       =      Local Lift coefficient

### 4.3.2 Load Distribution

$$\text{Load} = \text{Aerolift} - \text{Dead weight}$$

$$\text{Load distribution} = \text{Load} \times \text{Load Factor} \times \text{Safety Factor}$$

	STA [m]	Ci [m]	Strip Width [m]	W0 [N]	Wi [N]	Wavg [N]	Strip Load [N]	Total Shear [N]	Mom from Shear [N.m]	Wi+2W0 [N]	L0^2/6 [m]	Mom from Strip Load [N.m]	Total Moment [N.m]
1	0.88	0.1700						0	0.0000				0.0000
2	0.73	0.2000	0.15	1.90	2.24	2.07	0.31			6.04	0.0038	0.0226	0.0226
3	0.6	0.2114	0.13	2.24	2.36	2.30	0.30	0.31	0.0465			6.84	0.0028
4	0.5	0.2261	0.10	2.36	2.53	2.45	0.24		0.0792			7.26	0.0017
5	0.4	0.2409	0.10	2.53	2.69	2.61	0.26		0.0854			7.75	0.0017
6	0.36	0.3000	0.04	2.69	3.35	3.02	0.12		0.1115			8.74	0.0003
7	0.2	0.3000	0.16	3.35	3.35	3.35	0.54		0.0494			10.06	0.0043
8	0.1	0.3000	0.10	3.35	3.35	3.35	0.34		0.2836			10.06	0.0017
9	0	0.3000	0.10	3.35	3.35	3.35	0.34		0.2108			10.06	0.0168
								2.44	0.2444				1.0123

Table 17 : Dead Weight

	STA [m]	Ci [m]	Local Lift	Local Lift [N/m^2]	Wing Load per Meter [N/m]	Avg Running Load [N/m]	Strip Load [N]	Total Shear [N]	Mom Arm to Centroid [N]	Mom from Strip Load [N.m]	Total moment [N.m]
1	0.88	0.1700	0	0	0.00			0.00			0
						11.23	1.68		0.05	0.08	
2	0.73	0.2000	0.81454	112.2537938	22.45			1.68			0.08
						24.94	3.24		0.06	0.20	
3	0.6	0.2114	0.94179	129.7904344	27.43			4.93			0.51
						28.95	2.90		0.05	0.14	
4	0.5	0.2261	0.97783	134.7571969	30.47			7.82			1.14
						31.70	3.17		0.05	0.16	
5	0.4	0.2409	0.99186	136.6907063	32.93			10.99			2.08
						36.69	1.47		0.02	0.03	
6	0.36	0.3000	0.97815	134.8012969	40.44			12.46			2.55
						41.32	6.61		0.08	0.53	
7	0.2	0.3000	1.02057	140.6473031	42.19			19.07			5.07
						42.41	4.24		0.05	0.21	
8	0.1	0.3000	1.03077	142.0529906	42.62			23.31			7.19
						42.68	4.27		0.05	0.21	
9	0	0.3000	1.03364	142.4485125	42.73			27.58			9.73

Table 18 : Aero Lift

	STA [m]	Bending Moment [N.m]	Total Shear with Load Factor = 2.5 [N]	Total Moment with Load Factor = 2.5 [N.m]	Ultimate Bending [N.m]
1	0.88	0	0	0	0
2	0.73	0.06	3.433739416	0.153865047	0.230797571
3	0.6	0.4184	10.79234246	1.045950649	1.568925973
4	0.5	0.961933935	17.41911594	2.404834836	3.607252254
5	0.4	1.802241262	24.69172281	4.505603155	6.758404733
6	0.36	2.156420566	28.05781131	5.391051415	8.086577123
7	0.2	4.582624156	43.2428413	11.45656039	17.18484058
8	0.1	6.400870692	53.00542356	16.00217673	24.00326509
9	0	8.7176	62.83555117	21.79397826	32.6909674

Table 19 : Load Distribution

#### 4.3.3 Shear Force & Bending Moment Diagram

Due to demanding requirements of a lightweight but strong structure. Therefore, the structure must be designed utilizing optimization process. To determine whether the structure had sufficient strength, the wing bending moment must be defined. The value can be obtained from Shear & Bending moment diagrams.

Shear force diagrams is the summation of shear forces acting at each section across the aircraft wingspan. In which the shear force at the wingtip is 0. The value of the shear force at each section depends on the amounts of components and structural weight at that section. Shear force of the wing can be plotted as the following figure.

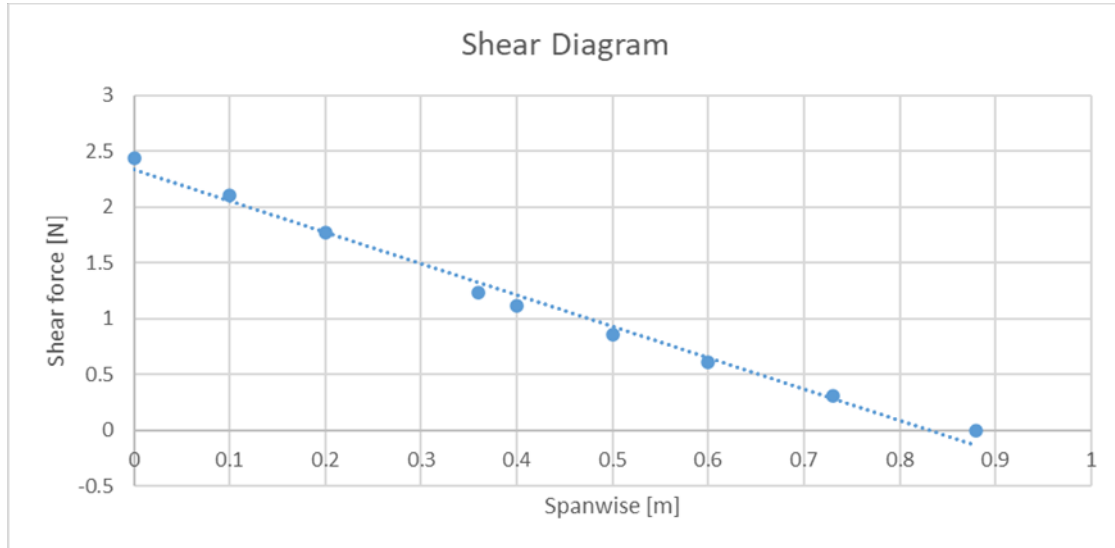


Figure 22 : Shear Diagram

Bending moment diagram can be generated by referring to the aforementioned span-wise shear force diagram. Wing bending moment can be calculated using the area under the span-wise shear force plot. Results as illustrated.

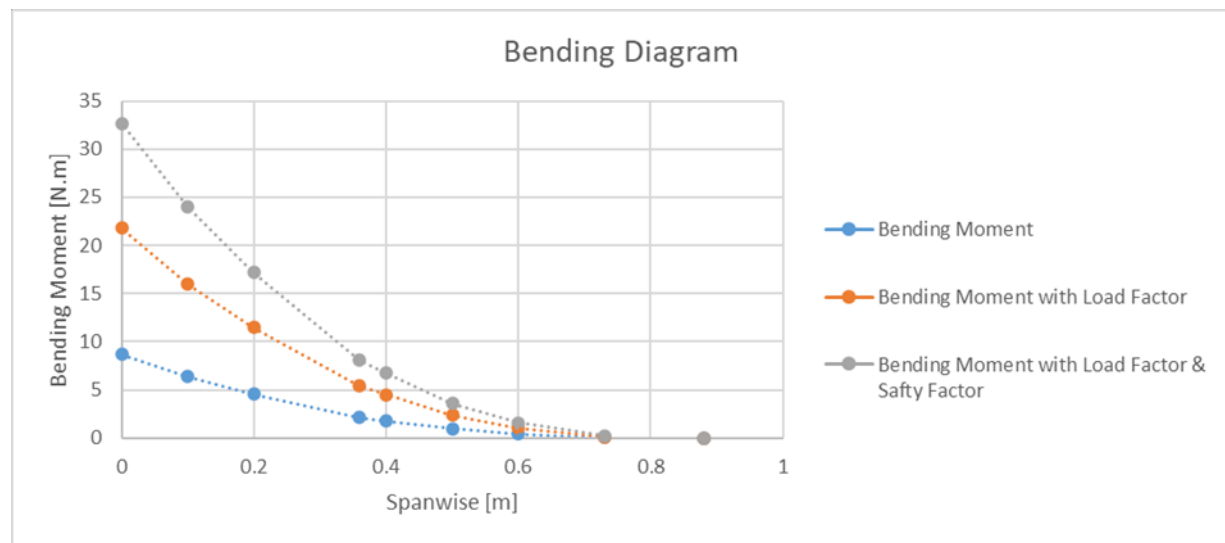


Figure 23 : Bending Diagram

#### 4.3.4 Position and Sizing of Spar

Generally, the wing structural part consists of front spar and rear spar. Front spar is mainly significant factor for overall structural reasons, such as bending and torsional stiffness; therefore maximum thickness location will provide highest moment of inertia also secondly consideration is about CP location. Placing spar in CP location should minimize moment arm and results to minimize load to structural parts consequently. For a rear spar, Significant consideration is only control surface location.

- **Control surface sizing**

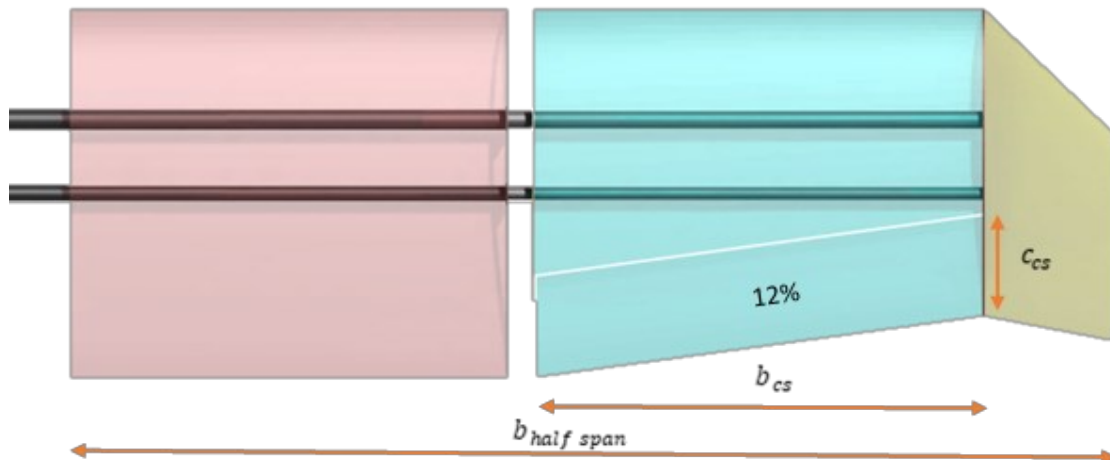


Figure 24 : Wing Semi Span

Based on previous designs for effective roll control of the aircraft. The area occupied by aileron is said to be 12% of the semi-span area of the wings. Which can be calculate using following formulae.

$$12\% = \frac{S_{cs}}{S_{wing}}$$

$$12\% = \frac{b_{cs} \times c_{cs}}{S_{wing}}$$

$$c_{cs} = 0.12 \times \frac{S_{wing}}{b_{cs}}$$

Where  $S_{wing}$  = Wing area (Can use Full span or Half span)

$S_{cs}$  = Control Surface Area

$b_{cs}$  = Span of Control Surface\*

$c_{cs}$  = Chord of Control Surface

\* In case, the ailerons were designed such that its span matches the span of the outer wing section.

From calculations, which yields  $c_{cs}$  of 0.08 meters. However, with rear spar positioned 0.08 meters from the wing trailing edge compromises wings strength and complicates manufacturing process. Therefore, the rear spar position is determined using the optimal depth from the wing surfaces at the airfoil section. Which results in rear spar position at 50% chord length from the wing leading edge. With similar criterion, front spar is located at maximum thickness of the airfoil. This configuration causes the moment of inertia of the wings to increase, thus, resulting in a lighter mass of the spars.

- **Spar Shape**

Shape of the wing spar structure depends on the bending stress. Which in 2 spars configuration, the stress is distributed between two spars. The magnitude of the stress shared on both spars depends on the distance of both spars to the center of pressure of the airfoil, in percent chord length. As shown in the figure below.

#### Moment Distribution Calculations of Front Spar and Rear

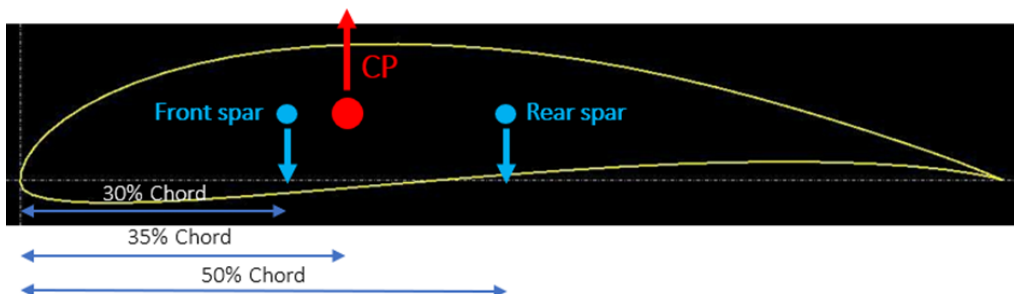


Figure 25 : Moment of Wing Spar

Assume Load at Center of Pressure = 100 %

Take moment at Front Spar.

$$\sum M = 0$$

$$100 \cdot (35 - 30) = R_{rs} \cdot (50 - 30)$$

Take moment at Rear Spar.

$$\sum M = 0$$

$$100 \cdot (50 - 35) = R_{fs} \cdot (50 - 30)$$

Where  $R_{fs}$  = Reaction of Front Spar

$R_{rs}$  = Reaction of Rear Spar

From calculations, the rear spar will support 25% of total load whereas the rest of the load is absorbed by the front spar. After determining the moment at each spar, moment of inertia of both spars can then be determined. Using the relation below.

Spar	Reaction Force [%]	Moment [N·m]	c [m]	Material	$\sigma$ [MPa]	Moment of Inertia [m <sup>4</sup> ]
Front spar	75	24.52	0.0238	Carbon fiber	570	$1.022 \times 10^{-9}$
Rear spar	25	8.17	0.0211	Carbon fiber	570	$3.021 \times 10^{-10}$

Table 20 : Spar Moment of Inertia

- Spar Dimension**

Our team chose hollow carbon fiber cylindrical spars out of other geometries due to the greatest optimization of the strength, market availability, and ease of manufacturability.

	Outer Diameter [mm]	Inner Diameter [mm]	Moment of Inertia [mm <sup>4</sup> ]	Moment of Inertia [m <sup>4</sup> ]	
<b>Hollow Circular</b>	16	14	1331.25	$1.33 \times 10^{-9}$	<b>Use for Front Spar</b>
	14	12	867.86	$8.67 \times 10^{-10}$	
	12	10	527.00	$5.27 \times 10^{-10}$	<b>Use for Rear Spar</b>
	10	8	289.81	$2.89 \times 10^{-10}$	

Table 21 : Hollow Circular Spar Moment of Inertia

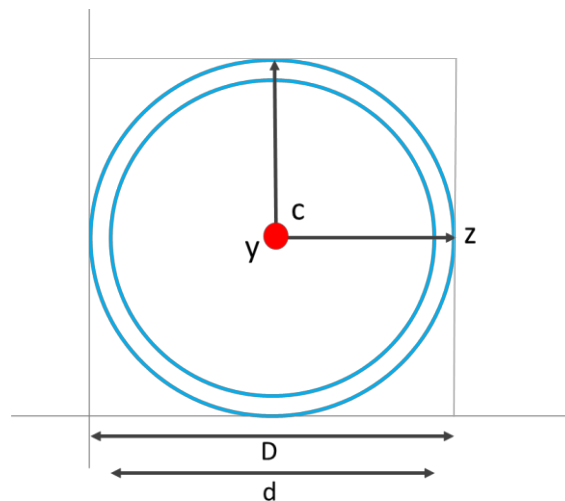


Figure 26 : Hollow Carbon Fiber Cylindrical

With the moment of inertia of both spars calculated. Optimal diameters of both front and rear spars can subsequently be obtained. The final calculation yield diameters of 16 mm and 12 mm, for front and rear spars, respectively.

## 4.4 Stability Analysis

### 4.4.1 Static Stability

Static stability is the initial tendency of the aircraft to return to its equilibrium state after a disturbance. We use xflr5 program to analyze the aircraft stability. To simplify an idealize model, fuselage effect was neglected in the stability analysis.

#### Longitudinal Axis

When we consider the aircraft pitching moment with respect to the angle of attack, the aircraft tends to generate positive pitching moment (clockwise) when the angle of attack is lower than trim angle and incase of angle of attack higher than trim angle, the aircraft produces negative pitching moment (counterclockwise). The trim condition of this aircraft is

approximately 2.5 deg and this aircraft pitching moment curve has negative slope ( $\frac{dC_m}{d\alpha} = -0.831 \text{ rad}^{-1}$ ) which indicates that the aircraft is in the longitudinal static equilibrium.

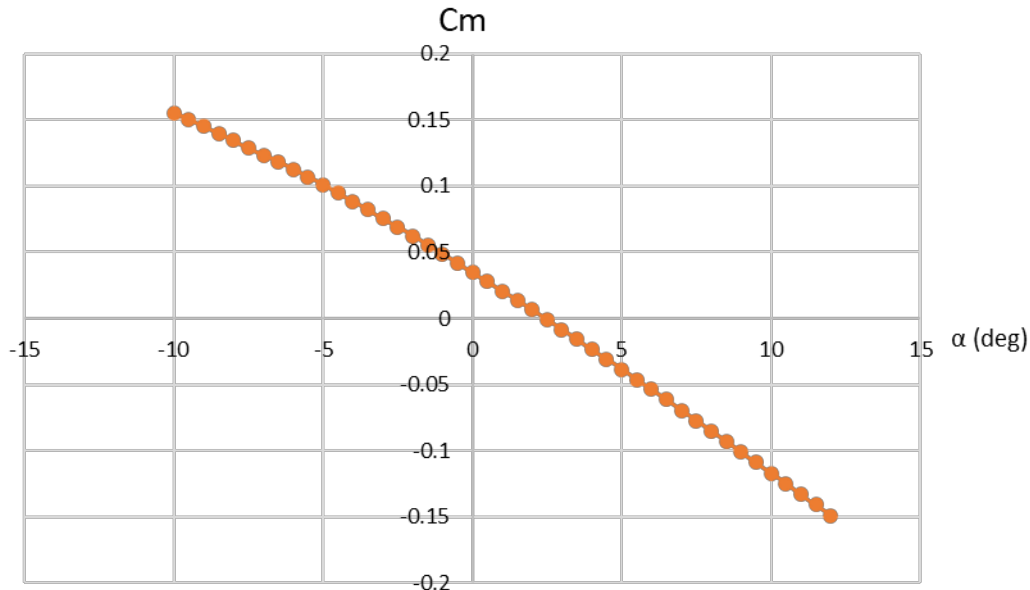


Figure 27 : Pitching Moment and Angle of Attack

### - Stick-Fixed Neutral Point

Static margin indicates the influence of center of gravity position on static stability with respect to neutral point. The aircraft center of gravity and neutral point are places at 0.105 and 0.154 m (figure 2) behind the wing leading edge, respectively.

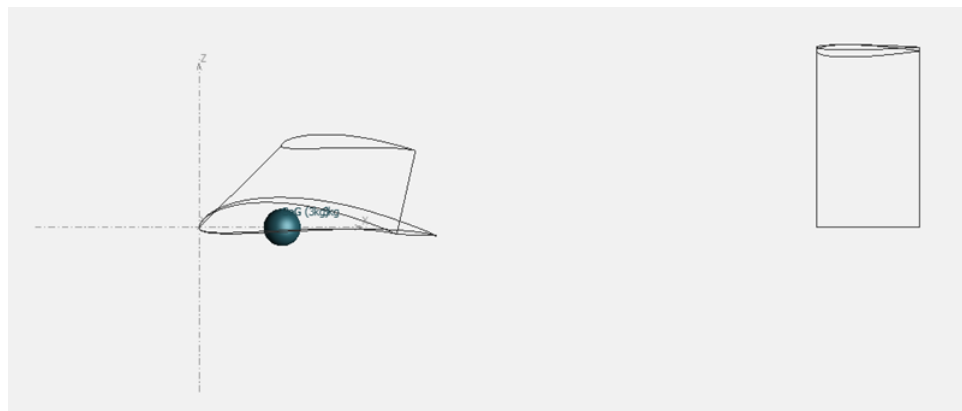


Figure 28 : Center of Gravity Position

The static margin can be determined by

$$\text{Static Margin} = \left( \frac{x_{NP}}{\bar{c}} - \frac{x_{cg}}{\bar{c}} \right)$$

When the mean aerodynamic chord is 0.278 m

$$\text{Static Margin} = \left( \frac{0.154}{0.278} - \frac{0.105}{0.278} \right)$$

$$\text{Static Margin} = 17.62 \%$$

The center of gravity is at 17.62% static margin where ahead of neutral point ( $x_{cg} < x_{NP}$ ), then the airplane is statically stable.

- **Lateral Axis**

From the rolling moment coefficient (Cl) plotted with respect to the sideslip angle ( $\beta$ ), the aircraft rolling moment curve has negative slope ( $\frac{dC_l}{d\beta} = -0.076 \text{ rad}^{-1}$ ) and intercepts at the origin point. The negative slope indicates that the roll moment created by sideslip rolls airplane back toward wings level attitude.

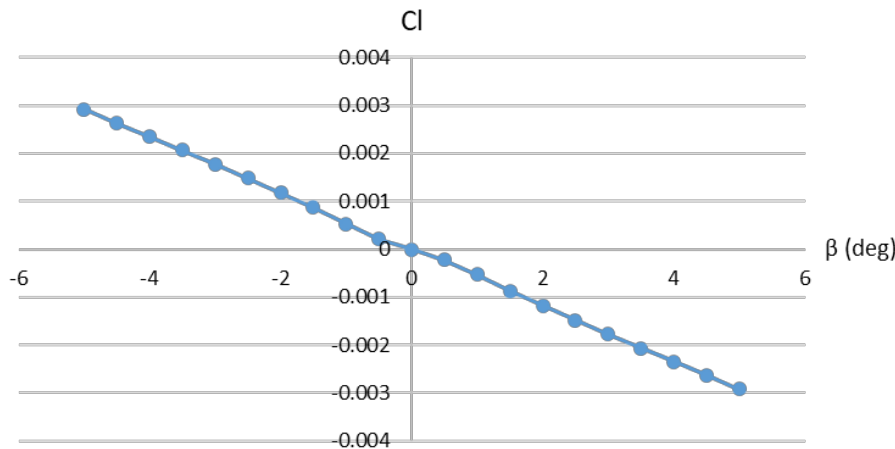


Figure 29 : Rolling Moment and Sideslip Angle

- **Directional Axis**

When we consider the yawing moment coefficient that varies with the sideslip angle, it generates the positive yawing moment curve slope ( $\frac{dC_n}{d\beta} = 0.102 \text{ rad}^{-1}$ ). The aircraft will develop a restoring moment that will tend to rotate the aircraft back to its equilibrium condition.

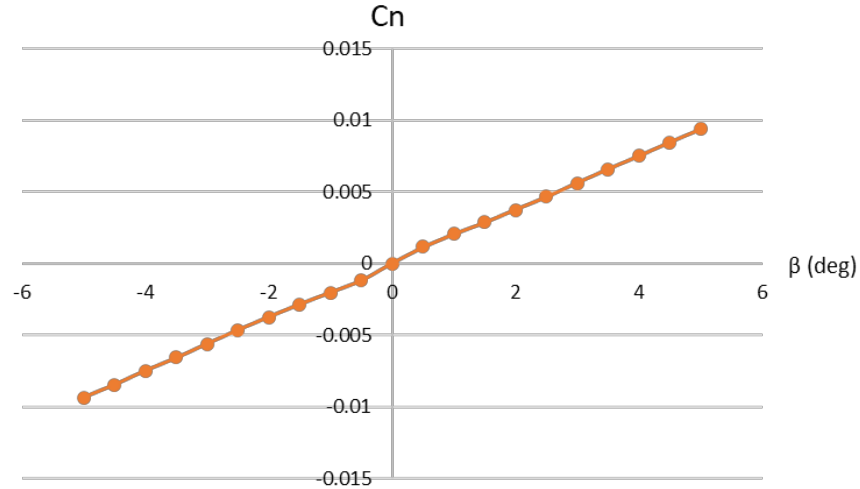


Figure 30 : Yawning Moment and Sideslip Angle

#### 4.4.2 Dynamic Stability

In addition to static stability, the aircraft also must be dynamically stable. An airplane can be dynamically stable if after being disturbed from its equilibrium flight condition the ensuing motion diminishes with time.

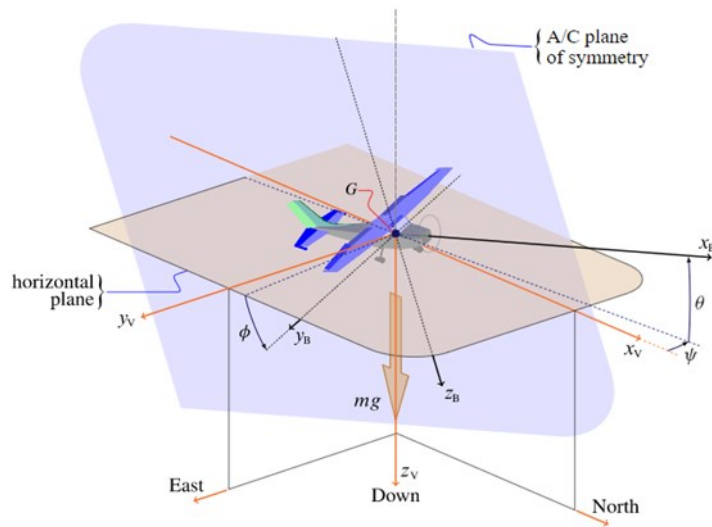


Figure 31 : Flight Dynamic Reference Frame

- **Stability Coefficients**

The aerodynamic force and moment can be represented by the stability coefficients in Table.

Longitudinal Stability Coefficients		Lateral Stability Coefficients	
$C_{X_u}$	-0.1111	$C_{Y_\beta}$	-0.43806
$C_{X_\alpha}$	0.49296	$C_{Y_p}$	-0.13334
$C_{Z_u}$	0.016562	$C_{Y_r}$	0.43674
$C_{L_\alpha}$	4.9305	$C_{l_\beta}$	-0.076327

$C_{Lq}$	8.4142	$C_{l_p}$	-0.46265
$C_{m_u}$	-0.0032211	$C_{l_r}$	0.22049
$C_{m_\alpha}$	-0.83101	$C_{n_\beta}$	0.10166
$C_{m_q}$	-12.465	$C_{n_p}$	-0.15981
		$C_{n_r}$	-0.12381

Table 22 : Stability Coefficient

- **Longitudinal Motion**

- **Longitudinal State Space Representation**

After we done the aircraft stability analysis from xflr5, the aircraft's equation of motion can be presented in the state-space form yields.

$$\begin{bmatrix} \Delta\dot{u} \\ \Delta\dot{w} \\ \Delta\dot{q} \\ \Delta\dot{\theta} \end{bmatrix} = \begin{bmatrix} -0.0914542 & 0.405804 & 0 & -9.81 \\ -1.50018 & -4.05873 & 11.9967 & 0 \\ -0.00953018 & -2.45869 & -5.13302 & 0 \\ 0 & 0 & 1 & 0 \end{bmatrix} \begin{bmatrix} \Delta u \\ \Delta w \\ \Delta q \\ \Delta \theta \end{bmatrix}$$

Where  $\Delta u$  is velocity along the x-axis

$\Delta w$  is velocity along the z-axis

$\Delta q$  is pitching velocity

$\Delta \theta$  is pitch angle

- **Longitudinal Approximation**

Parameter	Mode	
	Long-Period (Phugoid)	Short-Period
Eigenvalues, $\lambda$	$-0.0114 \pm j0.8389$	$-4.6302 \pm j5.4245$
Damping Ratio, $\zeta$	0.014	0.649
Natural Frequency, $\omega_n$ (Hz)	0.134	1.135
Damped Frequency, $\omega_d$ (Hz)	0.132	0.863

Table 23 : Longitudinal Dynamics Stability Parameters

- **Longitudinal Stability Root-Locus**

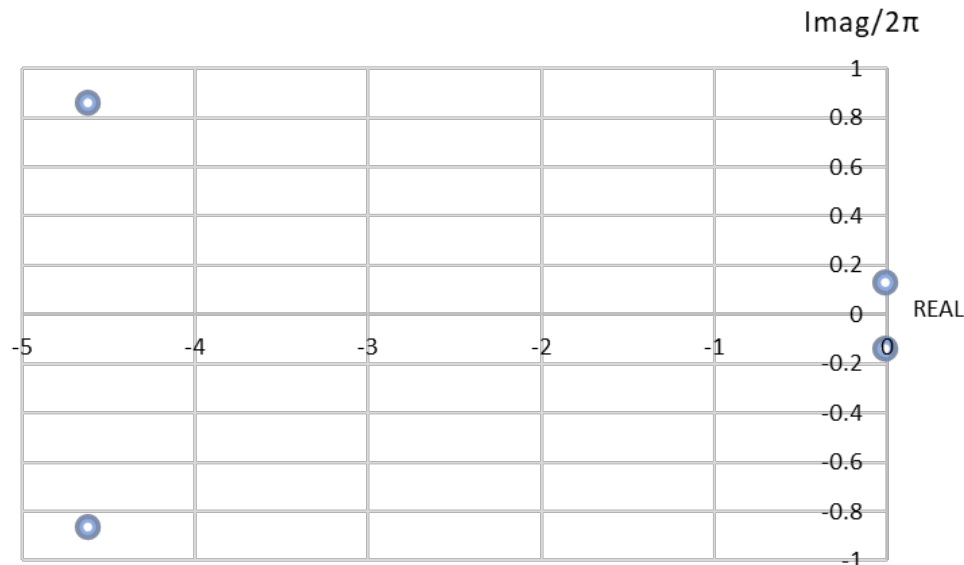


Figure 32 : Longitudinal Stability Root Locus

According to the longitudinal dynamic stability root locus plotted following the eigenvalues, all poles are located on the left side of s-plane (negative real part) that the aircraft has two symmetrical short-period and phugoid mode.

- **Lateral-Directional Motion**

- **Lateral-Directional State Space Representation**

$$\begin{bmatrix} \Delta\dot{v} \\ \Delta\dot{p} \\ \Delta\dot{r} \\ \Delta\dot{\phi} \end{bmatrix} = \begin{bmatrix} -0.360629 & -0.0917698 & -12.6601 & 9.81 \\ -1.48635 & -6.8705 & 3.4449 & 0 \\ 1.01723 & -0.839984 & -1.14459 & 0 \\ 0 & 1 & 0 & 0 \end{bmatrix} \begin{bmatrix} \Delta v \\ \Delta p \\ \Delta r \\ \Delta \phi \end{bmatrix}$$

Where  $\Delta v$  is velocity along the y-axis

$\Delta p$  is rolling velocity

$\Delta r$  is yawing velocity

$\Delta \phi$  is roll angle

### - Lateral- Directional Approximation

Parameter	Mode		
	Roll Damping	Dutch Roll	Spiral
Eigenvalues, $\lambda$	-7.1394	$-0.6879 \pm j4.1571$	0.1395
Damping Ratio, $\zeta$	-	0.163	-
Natural Frequency, $\omega_n$ (Hz)	-	0.671	-
Damped Frequency, $\omega_d$ (Hz)	-	0.662	-
Time to half amplitude (s)	0.097	-	-
Time to double amplitude (s)	-	-	4.968
Time Constant, $\tau$	0.140	-	-

Table 24 : Lateral Directional Stability Parameters

### - Lateral- Directional Stability Root Locus

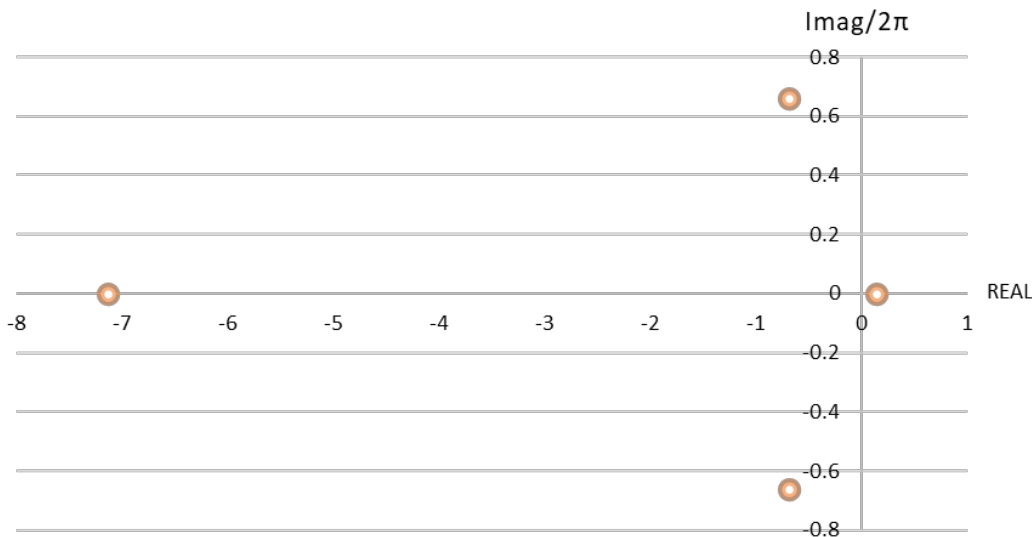


Figure 33 : Lateral Directional Stability Root Locus

When we plotted the lateral-directional stability root locus, it has three poles located on the left side of s-plane that stabilize the aircraft – one is placed on the negative real axes is the roll damping mode and the others on left side are Dutch roll mode. The other pole slightly placed on the s-plane's right side is the spiral mode that is unstable.

## 4.5 Antenna Tracker

Antenna tracker is used to determine the position of an aircraft by relaying GPS position and telemetry from the aircraft. It then uses this information to aim antenna towards the vehicle, while the vehicle is in flight.

#### 4.5.1 Antenna Tracker Hardware

- 900 MHZ 8 dBi Flat Patch Antenna



Figure 34 : Flat Patch Antenna

<b>Frequency</b>	902-928 MHz
<b>Gain</b>	8 dBi
<b>Horizontal Beam Width</b>	75 degrees
<b>Vertical Beam Width</b>	65 degrees
<b>Impedance</b>	50 Ohm

Table 25 : Electrical Specifications

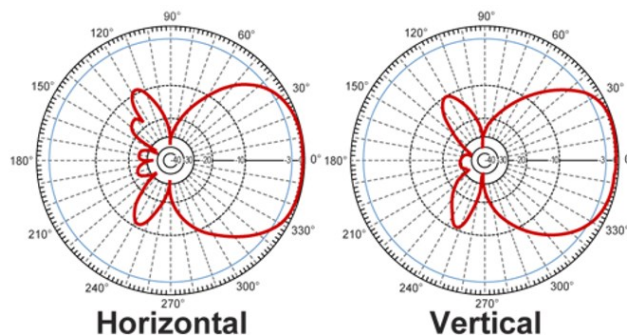


Figure 35 : Radio Frequency (RF) Antenna Gain Patterns

- Controller Pixhawk PX4 2.4.6



Figure 36 : Controller Pixhawk

- **Here 2 GNSS GPS Module**



Figure 37 : GPS Module

- **Horizontal and Vertical Servo (Torque = 40 kg.cm)**



Figure 38 : Servo

- **Long-Range UAV Telemetry Module 915 MHz**



Figure 39 : Long-Range Telemetry Module

#### 4.5.2 Antenna Tracker Assembly

The antenna tracker can be rotated horizontally (yaw) and vertically (pitch) using high torque servo as an actuator to move the mechanical part. To design the control system of antenna tracker, we use the Pixhawk PX4 controller and Here2 GPS module. Finally, the antenna tracker will track an aircraft by setting the control parameter using Mission Planner software e.g., PID value and Air Data and Attitude Heading Reference System (ADAHRS)

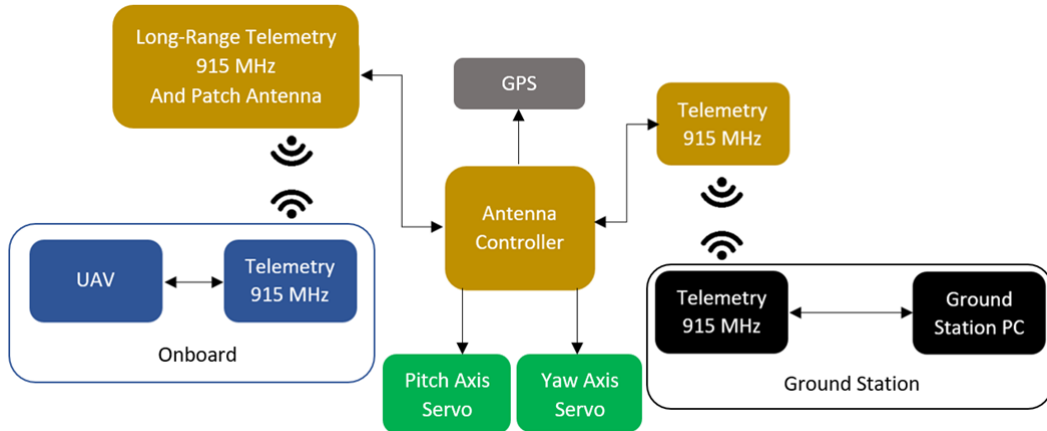


Figure 40 : Antenna Tracker and Telemetry Configuration

#### 4.6 Image Processing

The mission of AAVC 2021-2022 involves several targets, 2D animal figurines, printed on a 2X2 vinyl sheets. From the competition report guidelines, the target will be labeled with some markings where the team will need to visually confirm before dropping the mission payload. This stressed the importance of imaging system of our vehicle. According to mission descriptions, onboard imagery system shall be able to perform functions as follows.

- Search and locate the targets in the predetermined containment area.
- Obtain and relay all targets GPS coordinates.
- Provide a persistent image feed of the target along with its surroundings for 60 seconds.

#### 4.6.1 Composition of Imagery System

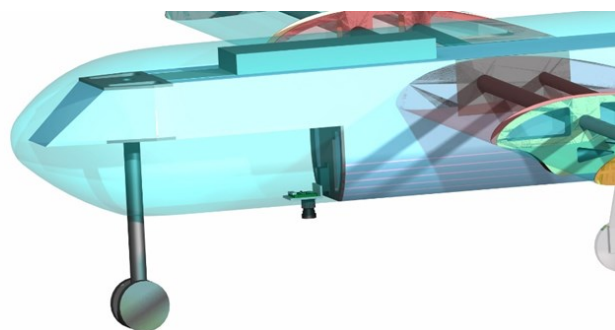


Figure 41 : Camera Bay Assembly, Microprocessor Units Located Above Fuselage Frame

To cope with the competition requirements, system must compose of the following hardware components.

- Camera
- Microprocessor
- Digital servo actuator(s)
- Wirings
- Antenna(s)
- Camera mount

#### 4.6.2 System Schematic

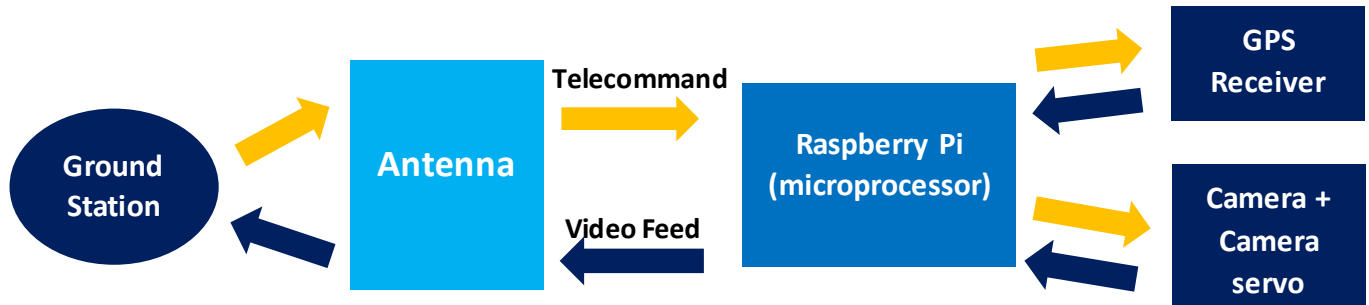


Figure 42 : Image Processing Configuration

#### 4.6.3 Camera



Figure 43 : Arducam 12MP HQ Camera, Isometric



Figure 44 : Front View



**ArduCam**



Figure 45 : Back View

Here, our team utilized off-the-shelf product from Arducam and purchased through authorized reseller. A HQ Raspberry Pi camera was chosen, with IMX 477 imaging sensor which enable for maximum resolution of 4056 x 3040 pixels (12.33MP). The IMX 477 sensor also possess colored image capabilities which would improve overall rate of success of the mission. Other relevant features as follow.

- Shutter type: Rolling Shutter
- IR Sensitivity: Visible light only
- Interface: MIPI
- Platform Support: Raspberry Pi

### HQ Camera

Mode	Resolution	Aspect Ratio	Frame rates	Video*	Image	FoV	Binning/ Scaling
1	2028 x 1080	169:90	0.1-50 fps	○		Partial	2 x 2 binned
2	2028 x 1520	4:3	0.1-50 fps	○		Full	2 x 2 binned
3	4056 x 3040	4:3	0.005-10 fps	○	○	Full	None
4	1012 x 760	4:3	50.1-120 fps	○	○	Full	4 x 4 scaled

Table 26 : Camera Capability

The camera is also capable of maximum frame rates up to 120 fps for its video mode; however, greater frame rate tends to compromise the resolution of the video feed. Therefore, optimization of both frame rate and video feed resolution will subsequently be tested for the best combination.

## Specs

- Sensor type: IMX477
- Pixel size: 1.55um x 1.55um
- Resolution: 4056(H) x 3040(V) 12.3MP
- Optical Size: 1/2.3"
- Lens spec: Focal length: 3.9mm, F.NO: 2.8, FOV: 75° (H), Low Distortion, M12 Mount(SKU:LN053), interchangeable
- Color Filter: 650nm
- Video Modes on Raspberry Pi: 1080p30, 720p60 and 640 × 480p60/90
- Interface Type: 2-lane MIPI
- Board Size: 24 x 25mm

*Figure 46 : Camera Specification*

To minimize contribution to the aircraft overall drag, the assembly is designed to be fully contained within the fuselage and possess minimal protrusion from the fuselage. With this approach, the drag contribution generated by imagery system is said to be greatly reduced. The camera will be mounted such that it has a perfect vertical top-down view, to maximize the field of view from level flight attitude.

### 4.6.4 Camera Mount & Servo

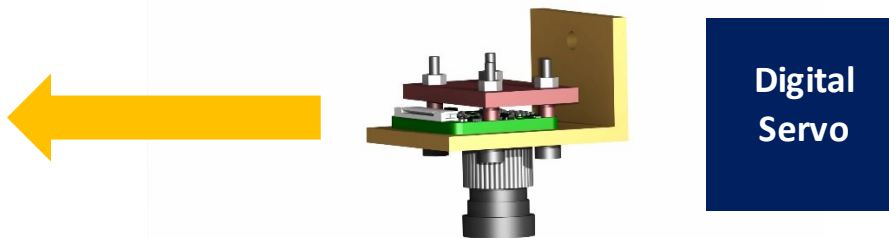


*Figure 47 : Camera Assembly, Arrow Indicates Direction Towards Nose of The Aircraft*

Camera mount ensures that the camera will be directed at the target. To reduce complexity and weight of the system our team have concluded that 1 degree-of-freedom motion camera mount is sufficient (panning motion only). While the additional tilt and zoom mechanism would result in the increase of weight with little merit, in which deemed such mechanisms unnecessary. The panning movement will be controlled via radio controller, which is remotely operated by ground station operator. Moreover, the digital servo responsible for the panning will be isolated from the microprocessor and connected to the Pixhawk flight controller. To ensure that maximum processing power is exclusively used for image processing only.



Figure 48 : Digital Servo Actuators

#### 4.6.5 GPS Receiver



Figure 49 : GPS Receiver Module

With the requirement of assigning GPS coordinates to every targets. GPS coordinates will be assigned to each target as per request by the ground station operator. Data from GPS receiver will be shared between flight path coordination and control system as well as on board imagery system. Such configuration will subsequently reduce the complexity and overall weight contribution inflicted on the total aircraft weight.

#### 4.6.6 Microprocessor



Figure 50 : Raspberry Pi Microprocessor, Isometric



Figure 51 : Top View

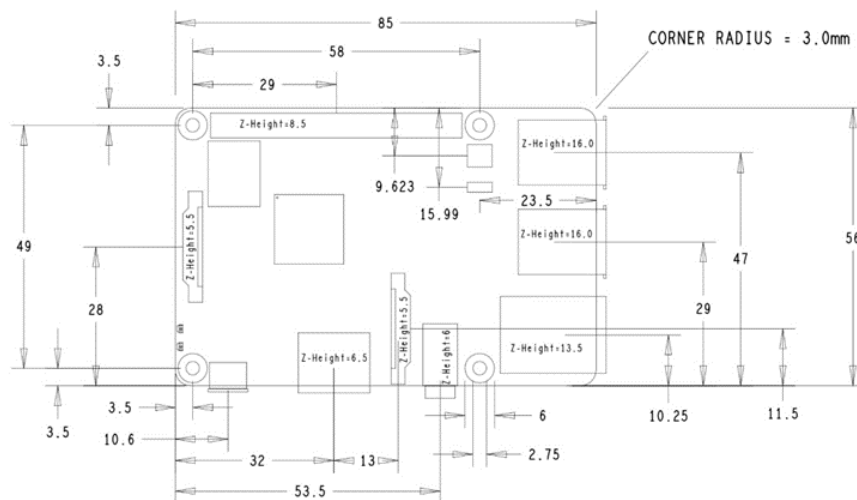


Figure 52 : Mechanical Drawing

Microprocessor board is the brain of the image processing system, for this mission, our team had decided to use a commonly available single board Raspberry Pi microprocessor. Based on previous experience of the team, microprocessors are more preferable than microcontroller boards due to greater performance of on-board processors. The Raspberry Pi board also has a built-in port dedicated for the use of camera, while most of the microprocessors would require an additional camera shield thus results in greater complexity and weight of the system.

A decision was made to completely isolate the use the microprocessor solely for image processing purposes only. As addition of components and functions to the system would hinder the limited processing capability of the microprocessor.



## Specifications

<b>Processor:</b>	Broadcom BCM2837B0, Cortex-A53 64-bit SoC @ 1.4GHz
<b>Memory:</b>	1GB LPDDR2 SDRAM
<b>Connectivity:</b>	<ul style="list-style-type: none"><li>■ 2.4GHz and 5GHz IEEE 802.11.b/g/n/ac wireless LAN, Bluetooth 4.2, BLE</li><li>■ Gigabit Ethernet over USB 2.0 (maximum throughput 300Mbps)</li><li>■ 4 x USB 2.0 ports</li></ul>
<b>Access:</b>	Extended 40-pin GPIO header
<b>Video &amp; sound:</b>	<ul style="list-style-type: none"><li>■ 1 x full size HDMI</li><li>■ MIPI DSI display port</li><li>■ MIPI CSI camera port</li><li>■ 4 pole stereo output and composite video port</li></ul>
<b>Multimedia:</b>	H.264, MPEG-4 decode (1080p30); H.264 encode (1080p30); OpenGL ES 1.1, 2.0 graphics
<b>SD card support:</b>	Micro SD format for loading operating system and data storage
<b>Input power:</b>	<ul style="list-style-type: none"><li>■ 5V/2.5A DC via micro USB connector</li><li>■ 5V DC via GPIO header</li><li>■ Power over Ethernet (PoE)-enabled (requires separate PoE HAT)</li></ul>
<b>Environment:</b>	Operating temperature, 0–50°C
<b>Compliance:</b>	For a full list of local and regional product approvals, please visit <a href="http://www.raspberrypi.org/products/raspberry-pi-3-model-b+">www.raspberrypi.org/products/raspberry-pi-3-model-b+</a>

Figure 53 : Microprocessor Specifications

### 4.6.7 Wirings

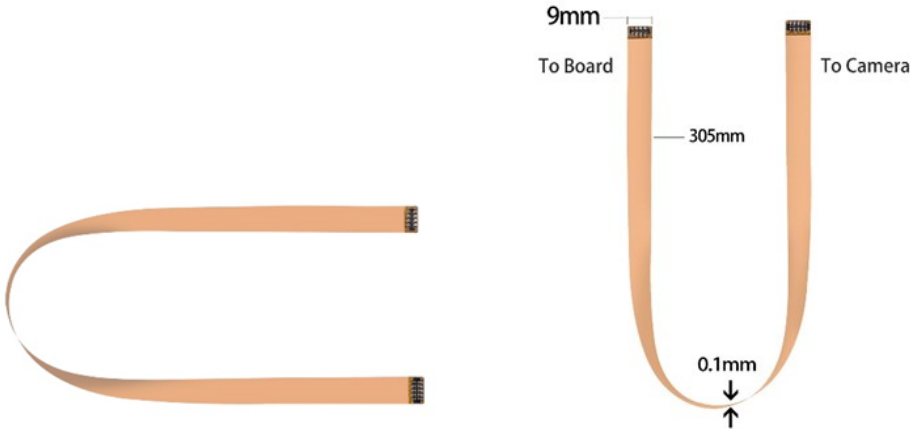


Figure 54 : Ribbon Cables

The system required 5V power for operation, in which the electricity will be introduced to the system via a USB type B connector. Due to its design, the microprocessor could power the camera with on-board power source. The camera would be connected to the Raspberry Pi with a ribbon cable, which powers the camera and provide means of data transfer from its sensors. Additional wirings for the antenna will also be incorporated to communicate and provide video feed interaction with ground station.

#### 4.6.8 Antennae



Figure 55 : Aomway Antenna

A separated set of antennas will be used for video feed transfer whilst the aircraft executes its mission, to ensure the least interference from radio controlled remote used by pilot. The antenna will be directly connected to the ground station display.

#### 4.6.9 Software

By using single board microprocessor, a variety of operating systems and software can be chosen for application. The Rasbian Operation System, developed by the Raspberry Pi Foundation, was chosen as the board operation system as it is the most compatible operation system for the selected microprocessor. Moreover, the said operating system is also readily available for installation from the internet with no additional cost, excluding the memory card that the operating system had been burnt onto. Raspberry Pi OS is one of the most versatile operating system available for the Raspberry Pi boards, as it is compatible with many programming languages such as: Java, C/C++, Python, and more.

As for image processing applications, our team concluded that Python programming language will be use, since all of group members had experience on this programming language. The coding will also be developed on the OpenCV program, which is compatible with all the hardware used in this mission and is available for download from the internet.

## 5.0 Manufacturing

After completion of detailed design, 3D model is generated in CATIA to get an overview of the components of UAV, in preparation for upcoming manufacturing process. The manufacturing method and materials selected for each UAV elements varies. As appropriate materials were selected to make the aircraft as light as possible. The manufacturing plan is divided by main component including fuselage, wing, tail, landing gear, camera system and payload system.

### 5.1 Material and Fabrication method selection

#### 5.1.1 Fuselage

The fuselage must be large enough to accommodate crucial components including 900 g water bottle (payload), electronics system, imagery system, and battery. Moreover, the fuselage must possess enough strength to withstand aerodynamic forces and moment from tail, wings, and impact force during landing without failure. The shape of the fuselage must facilitate drag reduction as much as possible and smooth surface finish to reduce skin friction.

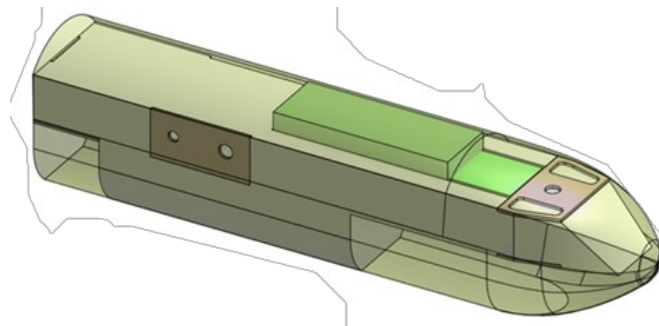


Figure 56 : Fuselage Model

The fuselage manufacturing process is divided into two parts which are fuselage structure and aerodynamic fairing. Each components possess different requirements for its material where materials with suitable material properties were chosen to match specific requirements; however, a common trait of high strength, lightweight and affordability can be found on both elements.

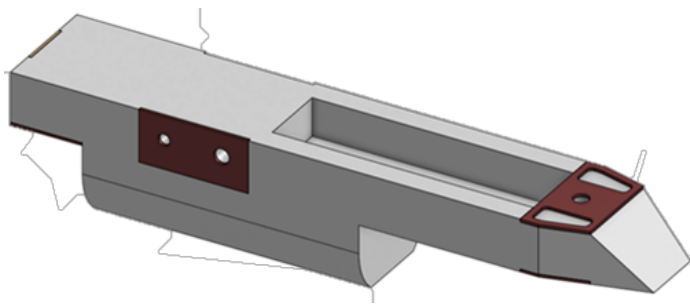
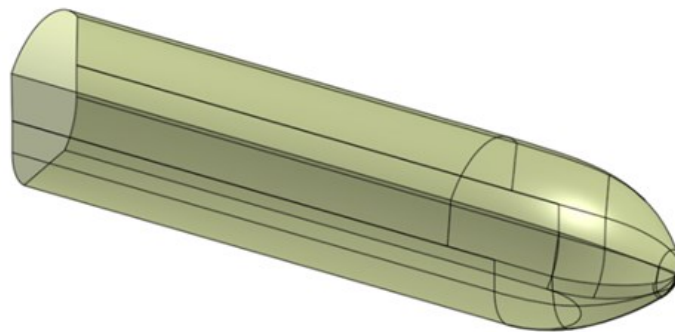


Figure 57 : Main Fuselage Structure

Main fuselage structure: Our team has concluded that Styrofoam will be primary material due to its lightweight, ease of manufacturability, and high market availability. In some locations, the fuselage structure will be reinforced with carbon fiber composite material or

laser-cut plywood. The reinforcing material depends on the criticality of the load such as structure located near the motor, wings, tail, and landing gear.



*Figure 58 : Aerodynamic Faring*

Aerodynamic fairing: Fiberglass composite material was selected due to its lightweight and high manufacturability when forming curved parts. Moreover, fiberglass fairings possess a smooth surface which aids the reduction of skin friction drag.

### **5.1.2 Wing and Empennage**

Wings and tail were regarded as two of most crucial elements of the UAV because they are components that occupy largest volume and space, which make significant impact to the aircraft characteristics, especially on weight.

Therefore, foam was selected due to its lightweight, ease of manufacturability, and easy to procure. Hot wire cutters are used to cut the foam into an airfoil shape, as well as fabrication of holes to accommodate spar structures and additional lightening holes. Additionally, the surface of the airfoils can be improved by coating with Oriented Polypropylene (OPP) tape, which lowers the contribution of skin friction drag of the components.

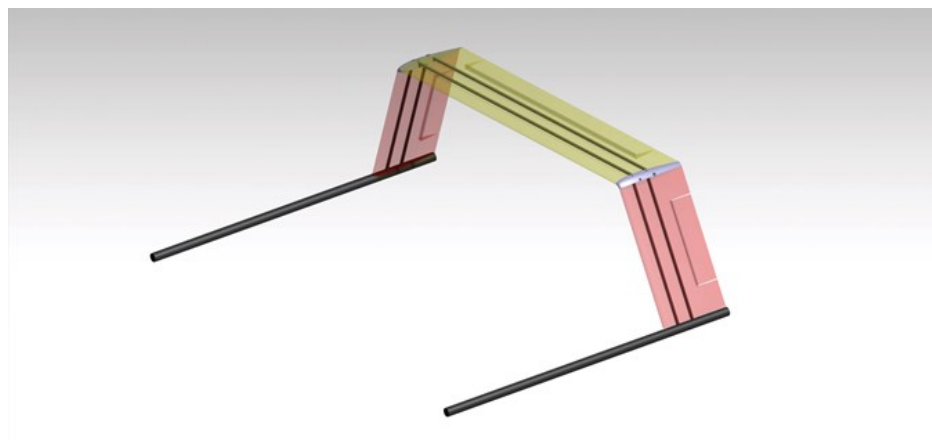


*Figure 59 : Twin-Boom Inverted U-Tail*

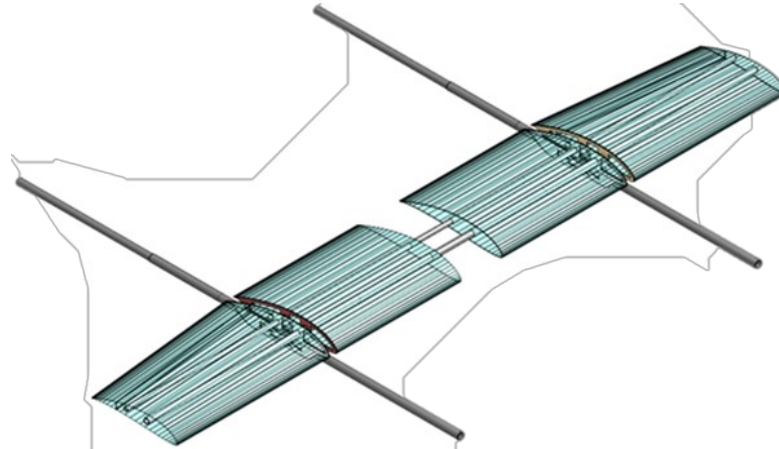


Figure 60 : Wing

Our UAV wings are divided into two parts: the inboard wing sections and the outboard wing sections. The inboard wing section was designed to be firmly fixed to the spar and fuselage by epoxy adhesives. While the outboard wing section was designed to be removable, as this design feature allows the UAV to be reconfigured for vertical take-off and landing configuration and aids ease of transportation. To achieve vertical take-off and landing capabilities, twin boom will be extended from the leading edge of the wing and allows for placement of 4 additional motors. As for fixed wing variant, the 4 motors and boom extension would be removed.

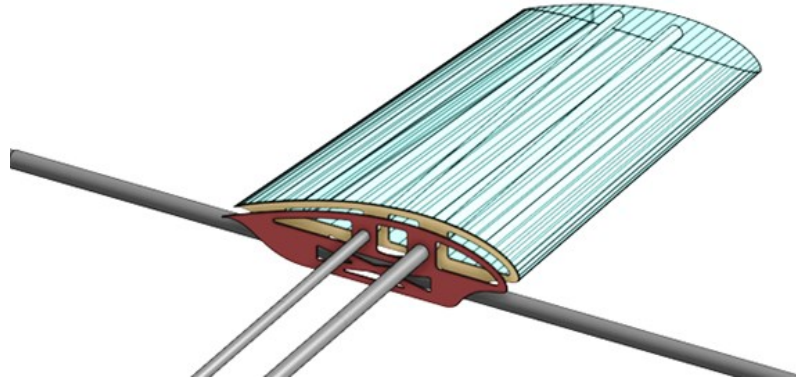


Figure 61 : Plywood Rib Part

At the wing-tail boom interface, additional laser-cut plywood ribs will be attached for additional strength. The ribs would also aids assembling accuracy; thus, UAV configuration changes can be done with ease.

### 5.1.3 Landing gear

Our team use heritage baseline landing gear to ensure that it works and reduces human error from manufacturing. With familiarity of the component, manufacturing speed can be improved.

#### 5.1.4 Imagery system

The camera assembly is attracted to the lower fuselage section. 3D printed camera mount and additional digital servo for support and panning movement.

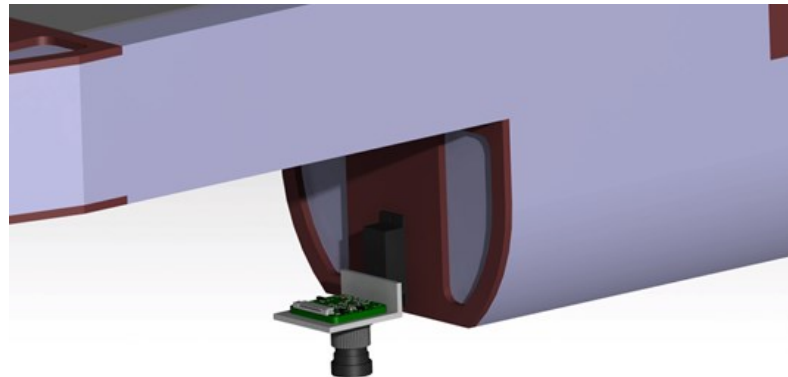


*Figure 62 : Camera Assembly*

#### 5.1.5 Payload system

The payload system will be completely contained within the UAV fuselage. The release mechanism servo is also installed so that payload can be discharged.

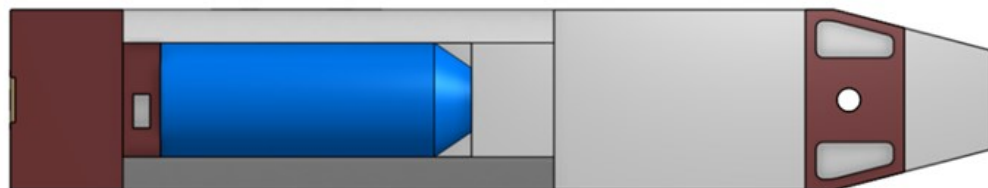


*Figure 63 : Payload System*

## 5.2 Manufacturing Plan

Milestone	July					August				
	1	7	15	25	31	1	5	15	25	31
<b>Fuselage</b>										
Laser cutting		■	■							
Hot wire cutting for fuselage structure			■	■						
Hand lay-up and vacuum for fuselage structure				■	■					
Hand lay-up and vacuum for fairing				■	■					
Assembly fuselage structure and fairing					■					
<b>Payload part</b>										
Laser cutting		■	■							
Assembly laser cut with fuselage				■	■	■				
servo mechanism							■	■		
<b>Camera part</b>										
Laser cutting and 3D printing		■	■							
Assembly laser cutting and 3D printing with fuselage		■	■							
Assembly camera part with fuselage								■	■	
<b>Wing</b>										
Laser cutting		■	■							
Hot wire cutting				■	■	■				
OPP tape coating						■				
Assembly wing component with carbon fiber tube spar						■	■			
<b>Tail</b>										
Hot wire cutting					■	■				
OPP tape coating						■	■			
Assembly tail with twin boom (carbon fiber tube)								■	■	
<b>Landing gear</b>										
Assembly landing gear part with fuselage								■	■	
<b>Assembly all component</b>									■	

Table 27 : Manufacturing Plan



### 5.3 Project Cost Breakdown Structure

Project cost breakdown structure (CBS) represents the various costs involved in a project. Which one of components in the Work Breakdown Structure (WBS). This table shows the cost breakdown structure of this UAV, which estimates total cost of a single unit. All expenses can be broken down into materials for building and repairing UAV, internal systems, and additional expenses such as travel expenses for training and system or UAV spare parts.

WBS Item	Cost (Bath)
<b>UAV Design</b>	
Aerodynamic	
Structure	
Stability	
Propulsion	-
Electronic Part	
Payload System	
<b>Total</b>	
<b>System Design</b>	
Flight Control System	27965
Image Processing System	7459
Antenna Tracker System	28650
<b>Total</b>	64074
<b>Manufacture</b>	
Fuselage	2000
Wing	3500
Tail	3000
<b>Total</b>	8500
<b>Integration</b>	
UAV Airframe	
Payload system	
Propulsion	
Electronic Part	-
Flight Control System	
Image Processing System	
Antenna Tracker System	
<b>Total</b>	0
<b>Testing</b>	
UAV Structure	
Payload drop mechanism	
Electronic Part	
Propulsion	2000
Flight Control System	
Image Processing System	
Antenna Tracker System	



Full System	
Test flight	
<b>Total</b>	<b>0</b>
<b>Member Training</b>	
Pilot Training	-
Equipment Training	-
<b>Total</b>	<b>0</b>
<b>Mission Operating Practice</b>	
Traveling Expenses	1000
<b>Total</b>	<b>1000</b>

Table 28 : Cost Breakdown Structure

## 6.0 Testing Plan

The aircraft will be tested to guarantee that components, subsystems, and assemblies were ready for competition and to generate experimental data for refinement of the UAV.

### 6.1 Testing objective and testing method

#### 6.1.1 Propulsion and Control system

The goal of propulsion and control system testing is to test that all components can work well, with good response to the pilot input and no interruption when the aircraft is in operation.

No	Components	Testing Goal	Testing Method
1	Battery	<ul style="list-style-type: none"> <li>- The battery must not overheat after the flight.</li> <li>- The battery can resist high voltage demand from the motor instantaneously.</li> </ul>	<ul style="list-style-type: none"> <li>- The voltage and endurance will be monitored while operating with a fixed current. The best performing battery packs were marked so that they could be used for test flights.</li> </ul>
2	Propeller and Motor	<ul style="list-style-type: none"> <li>- The motor and propeller should create sufficient thrust for the aircraft.</li> <li>- The temperature of the motor must not exceed the limit set by the manufacturer.</li> <li>- The current and voltage must not exceed the limit when operate in the maximum throttle regime.</li> <li>- There are no strange sound and high vibration with the motor. Which indicates that the motor does not work properly.</li> </ul>	<ul style="list-style-type: none"> <li>- The motor will be tested on the static thrust stand with the propeller and constant power supply.</li> <li>- The propellers were tested on the static thrust stand along with the motor and constant power supply. The propeller tests will verify the performance and selection of the propeller.</li> </ul>
3	Servo	<ul style="list-style-type: none"> <li>- Servos provide enough torque for control the control surface and resist aerodynamic forces.</li> <li>- Servo has long life cycle and servo gear does not wear easily.</li> <li>- The servo has enough arm angle as required.</li> </ul>	<ul style="list-style-type: none"> <li>- Supply power to servo and control servo with a transmitter, then, observe movement of the servo arm.</li> </ul>
4	Receiver	<ul style="list-style-type: none"> <li>- The receiver has sufficient channels for control all devices.</li> <li>- Receiver possesses enough range for competition and maintains connection with the transmitter.</li> </ul>	<ul style="list-style-type: none"> <li>- Test range with a range test mode on ground.</li> <li>- Test range in-flight and check control signal regardless of direction of aircraft and transmitter antenna.</li> </ul>

Table 29 : Testing Goal of Each Component in Propulsion and Control System



### 6.1.2 Wing and Spar

The wing spars were designed and handle bending stress. Maximum load tests will be conducted on the wings with sandbags. The wings were supported on their tips while the structure was loaded with weights, distributed along the spar. Wings will be tested until they exceeded the maximum predicted bending stress.

### 6.1.3 Landing Gear

The landing gear will be tested to examine strength of landing gear and wheel. The team will control the full-loaded aircraft to perform touch and go with varying landing speed, then collect the data and adjust the landing gear from videos and other data recordings.

### 6.1.4 Payload Drop System

The Payload Drop System is tested to guarantee that the payload drop mechanism can operate under maximum payload weight conditions and retain smooth operation when the aircraft is in flight.

### 6.1.5 Performance

The performance will be calculated with flight mechanics equations. The important performance is cruise speed, takeoff field length, stall speed, and stability characteristic of the aircraft. After performance calculations, the team will verify the actual performance by installing the Pixhawk Flight Controller to the aircraft temporarily and perform a flight test, then obtain the log file from the flight controller for further analysis.

### 6.1.6 Flight Tests

To evaluate the overall performance of the aircraft, flight tests were performed with a telemetry system on board. Flight test objectives will be outlined before test flight dates. These objectives included trimming, pilot control feedback, completing all missions, and monitor the performance points.

## 6.2 Flight Test Schedule

The testing of prototype aircraft will commence from August 2021 to September 2021. The testing plan and objective of each flight test shown in Table.

Test	Objective	Date
Propulsion and Control system	Static thrust performance tests with motor, propeller, and battery packs.	15 August 2021
Wing and Spar	Verify spar meets bending stress requirements.	28 August 2021
Landing Gear	Impact Testing to simulate hard landing.	29 August 2021
Payload Drop System	Ensure that can be operated in maximum payload weight and no interruption when the aircraft operate in flights.	29 August 2021



Performance	Test and measure performance, aerodynamics, and stability characteristic of aircraft.	11 September 2021
Flight Tests	Compare flight measurements to calculated model.	12 September 2021

Table 30 : Flight Test Schedule

### 6.3 Pre-flight Checklist

Pre-flight check is the procedure to verify overall readiness of the aircraft before execution of flights. This checklist will perform at the beginning of every flight to ensure safety of the aircraft and operators. This list is also used conjunctually for maintenance of the aircraft. The checklist includes inspection procedures of all components.

Pre-Flight checklist	
<b>Structural Integrity – Visual inspection for damaged components</b>	
<input type="checkbox"/> Wing	<input type="checkbox"/> Landing Gear
<input type="checkbox"/> Boom	<input type="checkbox"/> Nose Gear
<input type="checkbox"/> Control Surfaces	<input type="checkbox"/> Fuselage
<input type="checkbox"/> Payload Drop System	<input type="checkbox"/> Motor Mount
<input type="checkbox"/> Propeller	<input type="checkbox"/> Boom
<b>Avionics – Ensure all wires and electrical components are connected and performing properly</b>	
<input type="checkbox"/> Servo Wiring	<input type="checkbox"/> Receiver Properly Connected
<input type="checkbox"/> Avionic Power Test	<input type="checkbox"/> Receiver Battery Peaked
<input type="checkbox"/> Servo Test	<input type="checkbox"/> Main Battery Peaked
<b>Propulsion – System should perform as desired</b>	
<input type="checkbox"/> Motor Wiring	<input type="checkbox"/> Prop Clearance
<input type="checkbox"/> Battery Connected	<input type="checkbox"/> Motor Test
<b>Final Inspection – Ensure safe, successful flight</b>	
<input type="checkbox"/> Correct Control Surface Movement	<input type="checkbox"/> Ground Crew Clear
<input type="checkbox"/> Mission / Objective Restated	<input type="checkbox"/> Pilot and Spotter Ready

Table 31 : Pre Flight Checklist



## 7.0 Appendix

Cost estimation of all equipment and materials based on information from our past UAV designs. The estimated cost of each respective components of the UAV is shown in table.

Description	QTY	Unit Price (Bath)	Total (Bath)
<b>UAV</b>			
OPP Tape 2"	6	45	270
UHU POR	2	95	190
Epoxy Glue	2	110	220
Balsa Wood 1.5mm	2	50	100
PVC Foam board	6	495	2970
Carbon fiber tube 10"	4	440	1760
Carbon fiber tube 12"	4	500	2000
Carbon fiber tube 14"	4	550	2200
Carbon fiber tube 16"	4	670	2680
Landing Gear	1	354	354
<b>Composite Part</b>			
Sealant Tape	1	300	300
Peelpy (1.5x5m)	1	480	480
Breather Fabrics (1.5x5m)	1	525	525
Bagging Film (4x3m)	1	480	480
FiberGlass Fabric	1	240	240
Carbonfiber Fabric 1.5x3m	1	3,900	3900
Epoxy Resin Part A&B	1	780	780
<b>UAV Electronic Part and Flight Control</b>			
Motor	1	1350	1350
Motor (VTOL)	4	952	3808
Horizontal Thrust Propeller	1	204	204
Vertical Lift Propeller (VTOL)	4	412	1648
Receiver	1	950	950
ESC	1	990	990
Vertical Lift ESC (VTOL)	4	320	1280
Servo	5	646	3230
Vertical Lift Servo (VTOL)	4	353	1412
UAV Vertical Lift Motor Mount	4	150	600
horn	1	250	250
Li-Po Battery (VTOL)	1	6400	6400
Servo cable	1	490	490
APM Power module	1	133	133
PixHawk Autopilot	1	2597	2597
GPS module	1	793	793
Air/Ground telemetry module	1	1468	1468

Buzzer/safety switch	1	143	143
Pitot tube	1	219	219
<b>Antenna Tracker</b>			
900 MHz 8 dBi Flat Patch Antenna	1	2493	2493
Servo	2	2122	4244
Pixhawk PX4 2.4.6	1	4633	4633
Tripod	1	1990	1990
Battery 1500mAh	1	415	415
Long Range UAV Telemetry	1	11427	11427
GPS	1	3970	3970
Telemetry Module	1	1468	1468
Indoor Signal Booster	1	3260	3260
<b>Image System</b>			
Raspberry Pi	1	2700	2700
HQ Camera	1	2900	2900
Ribbon Cables	1	250	250
Aomway	1	1609	1609
			<b>89073</b>

Table 32 : Cost Estimation

Final unit cost is 89,073 baht, which is an estimated cost for building one UAV. Which includes cost of electronical components, flight control, image processing system and antenna tracker.